

# Temperature Dual Enantioselective Control in a Rhodium-Catalyzed Michael Type Friedel-Crafts Reaction: A Mechanistic Explanation

Isabel Méndez,<sup>[a]</sup> Ricardo Rodríguez,<sup>\*[a]</sup> Víctor Polo,<sup>[b]</sup> Vincenzo Passarelli,<sup>[a],[c]</sup> Fernando J. Lahoz,<sup>[a]</sup> Pilar García-Orduña<sup>[a]</sup> and Daniel Carmona<sup>\*[a]</sup>

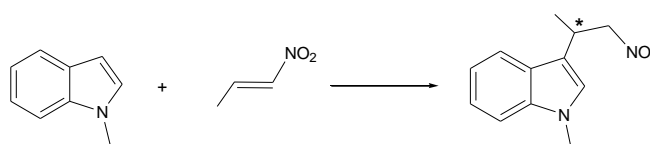
**Abstract:** By changing temperature from 283 K to 233 K, the *S* (99 % ee) or the *R* (96 % ee) enantiomer of the Friedel-Crafts (FC) adduct of the reaction between *N*-methyl-2-methylindole and *trans*- $\beta$ -nitrostyrene can be obtained by using ( $S_{Rh}$ ,  $R_C$ )-[( $\eta^5$ -C<sub>5</sub>Me<sub>5</sub>)Rh((*R*)-Prophos)(H<sub>2</sub>O)][SbF<sub>6</sub>]<sub>2</sub> as catalyst precursor. This catalytic system presents two other uncommon features: i) the ee changes over the reaction time with trends that depend on the reaction temperature and ii) an increase of the catalyst loading results in a decrease of the ee in the *S* enantiomer. Detection and characterization of the intermediates metal-nitroalkene and metal-*aci*-nitro complexes, free *aci*-nitro compound and FC adduct-complex, together with solution NMR measurements, theoretical calculations and kinetic studies allow us to propose two plausible alternative catalytic cycles. On the basis of these cycles all the above mentioned observations can be rationalized. In particular, the reversibility of one of the cycles together with a kinetic resolution in the intermediate *aci*-nitro complexes account for the high ee achieved in both antipodes. On the other hand, kinetic measurements explain the unusual effect of the increment in catalyst loading.

## Introduction

One of the most efficient methodologies for the preparation of enantioenriched compounds is based on the employ of transition-metal complexes as asymmetric catalysts.<sup>[1]</sup> In this approach, the synthesis of both enantiomers of a target chiral molecule, an increasingly desirable goal, usually requires the preparation of both enantiomers of a chiral catalyst. However, many catalysts are only readily available in a single configuration.

Enantiodivergent catalysis circumvents this problem by exploiting the chirality of a single enantiomer catalyst to produce both antipodes of a desired product.<sup>[2]</sup> This methodology can be implemented by altering the metal or the counter ion, by employing achiral additives, or by changing the reaction conditions. Among the latter, reaction temperature, a parameter that can be easily modified, constitutes an ideal variable to tackle the enantiodifferentiation of prochiral compounds. However, in transition-metal catalyzed processes, only a few reports of dual enantioselectivity being controlled by changing temperature have been published up to now and only moderate degrees of stereoselection, in one or in both enantiomers, have been achieved.<sup>[3,4]</sup> Moreover, in most cases, experimental observations and theoretical calculations that might help to explain the observed dual stereocontrol are scarce and therefore, mechanistic rationales for this switch of enantioselectivity are often not well understood.

On the other hand, the catalytic asymmetric Friedel-Crafts (FC) alkylation of aromatic substrates with electron-deficient alkenes is a key reaction in synthetic organic chemistry that enables the formation of new C-C bonds.<sup>[5]</sup> In particular, it provides an efficient methodology for the asymmetric functionalization of indoles leading to valuable biologically active derivatives.<sup>[6]</sup> In this context, the Michael-type asymmetric FC alkylation reaction of indoles with nitroalkenes<sup>[7]</sup> is especially important because, after the addition has taken place, the resulting nitro-indole compounds (Scheme 1) may be easily converted into biologically important derivatives such as tryptamines,  $\beta$ -carbolines or indole alkaloids.<sup>[6]</sup>



**Scheme 1.** Alkylation of Indoles with Nitroalkenes

Transition-metal complexes efficiently catalyze the alkylation of indoles with nitroalkenes. In 2005, Bandini *et al.* reported that an Al(Salen) compound mediated the stereoselective addition of indoles to aromatic nitroolefins.<sup>[8]</sup> Subsequently, several homogeneous metallic systems based on copper<sup>[9]</sup> (including a Cu<sub>2</sub>/Eu derivative)<sup>[10]</sup> or zinc<sup>[11]</sup> and, to a lesser extent, nickel,<sup>[12]</sup> platinum<sup>[13]</sup> or palladium,<sup>[14]</sup> were successfully applied to this

[a] Dr. I. Méndez, Dr. R. Rodríguez, Dr. V. Passarelli, Prof. Dr. F. J. Lahoz, Dr. P. García-Orduña, Prof. Dr. D. Carmona  
Departamento de Catálisis y Procesos Catalíticos  
Instituto de Síntesis Química y Catálisis Homogénea (ISQCH),  
CSIC - Universidad de Zaragoza  
Pedro Cerbuna 12, 50009 Zaragoza, Spain  
E-mail: dcarmona@unizar.es

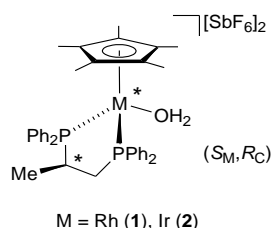
[b] Dr. V. Polo  
Departamento de Química Física  
Universidad de Zaragoza  
Pedro Cerbuna 12, 50009 Zaragoza, Spain

[c] Dr. V. Passarelli  
Centro Universitario de la Defensa  
Ctra. Huesca s/n, 50090 Zaragoza, Spain

Supporting Information for this article is given via a link at the end of the document.

transformation in combination with bis-oxazoline type ligands which are by far the most employed chiral ligands in these catalytic processes. In some cases, high conversions and good enantioselectivities were achieved but reliable mechanistic information is scarce. Usually, catalysts are generated *in situ* by mixing a catalyst precursor with the chiral ligand and no details about the metallic intermediates involved in the catalysis were depicted. In fact, neither experimental studies nor theoretical calculations dealing with the catalytic systems have been reported so far and the proposed transition states and catalytic cycles mostly rely on the stereochemistry determined for the reaction products.

Some years ago, we reported the preparation and characterization of the chiral half sandwich rhodium and iridium complexes  $(S_M, R_C)-[(\eta^5-C_5Me_5)M\{(R)\text{-Prophos}\}(H_2O)][SbF_6]_2$  [Prophos = propane-1,2-diyl-bis(diphenylphosphane)]; M = Rh (**1**), Ir (**2**) (Scheme 2).<sup>[15]</sup> These complexes easily lose the coordinated water molecule and it has been shown that the resulting unsaturated Lewis-acid cations are active and stereoselective catalysts for Diels-Alder<sup>[16]</sup> and 1,3-dipolar<sup>[15,17]</sup> cycloadditions as well as, for the FC reaction between 1,3,5-trimethoxybenzene and *trans*- $\beta$ -nitrostyrenes.<sup>[18]</sup> Furthermore, this system is well suited to study metallic intermediates involved in the catalytic processes such as nucleophile-catalyst<sup>f[15b,16a-c,17b-d]</sup> or adduct-catalyst<sup>f[16d]</sup> complexes.



**Scheme 2.** Chiral Complexes  $[(\eta^5-C_5Me_5)M\{(R)\text{-Prophos}\}(H_2O)][SbF_6]_2$

With all the above mentioned concerns in mind, we envisaged the possibility of applying complexes **1** and **2** as catalyst precursors for the FC reaction between indoles and *trans*- $\beta$ -nitrostyrenes, with the aim of obtaining a deeper insight into the mechanism of the catalytic process. During our preliminary explorations, we found that the metallic compounds **1** and **2** were active and selective catalysts for the above mentioned FC addition but, unexpectedly, we also observed that the values and sign of the enantioselectivity were strikingly dependent on the temperature, the catalyst loading and the reaction time.

Herein we report on the spectroscopic, kinetic and theoretical studies carried out to disclose the mechanism of this FC reaction and to explain the relationship between the reaction conditions and enantioselectivity. The whole body of collected data allows us to propose a plausible catalytic cycle for the FC reaction between indoles and *trans*- $\beta$ -nitrostyrenes and to rationalize the experimental outcome of the catalysis.

Part of this work has been previously communicated.<sup>[19]</sup>

## Results and Discussion

### Catalytic reactions

Complexes **1** and **2** efficiently catalyze the reaction between indoles and *trans*- $\beta$ -nitrostyrenes. Table 1 gathers a selection of the obtained results together with the reaction conditions. All the performed catalytic runs are presented in Tables S1-S7 of the Supporting Information (SI). The collected results are the average of at least two comparable reaction runs. Reactions were carried out in  $CH_2Cl_2$ , at 298 K in the presence of 4Å molecular sieves. A molar ratio  $cat^*/nitroalkene/indole$  of 1/30/20 (5 mol % catalyst loading) was employed in all cases. Catalytic runs were quenched after 30 minutes of reaction by adding excess of a saturated solution of  $N(nBu_4)Br$  in methanol. Reactions are clean: only the addition product and the remaining unreacted reagents were detected in the NMR spectra of the crude reaction mixture. The crystal structures of the adducts **3w** (entries 31, 32), **3x** (entries 33, 34) and **3ah** (entry 38) confirm the formation of the proposed products (see SI). Isolated yields are included for the adducts derived from *N*-methyl-2-methylindole (see Table S7, SI).

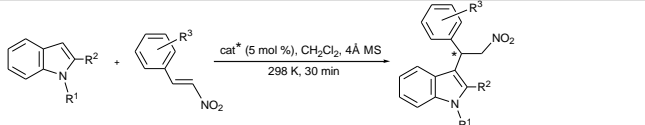
The rhodium system is more active than the iridium one but both metals exhibit TOFs from one to two orders of magnitude greater than those reported in the literature for the same reaction catalyzed by other metallic systems<sup>[8-14]</sup> (see Table S6, SI). No obvious relationships can be established between the stereoelectronic nature of the substituents, in both indole and nitroalkene, and the outcome of the catalytic reaction. With a few exceptions, enantioselectivities range from low to moderate. Changes in the enantioselectivity sign (entries 15-20 and 27-32) indicate that the opposite enantiomer was preferentially obtained by changing the metal.

Taking into account these results, we chose the reaction between *N*-methyl-2-methylindole and *trans*- $\beta$ -nitrostyrene catalyzed by the rhodium complex **1** (entry 27, quantitative conversion in 5 min and 98 % ee), to study the influence of the different reaction parameters on the catalysis. We started by assigning the absolute configuration to the resulting FC product **3u**.

### Determination of the absolute configuration of **3u**

The absolute configuration of the product derived from the reaction between *N*-methyl-2-methylindole and *trans*- $\beta$ -nitrostyrene was determined through the sequence of reactions depicted in Scheme 3.

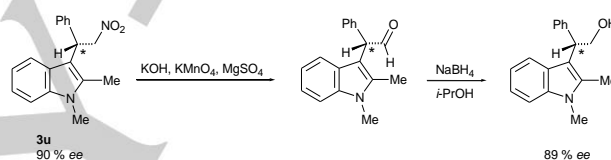
The nitro group was transformed into aldehyde following a variation<sup>[20]</sup> of the procedure reported by Nef.<sup>[21]</sup> The resulting aldehyde was reduced by *in situ* treatment with  $NaBH_4$  in 2-propanol. The absolute configuration *S* was assigned to the major FC adduct, by comparison of the optical properties of the obtained alcohol with those reported in the literature,<sup>[22]</sup> assuming that the configuration of the carbon center is retained over the whole determination process.

**Table 1.** Selected Asymmetric FC Alkylation Reactions of Indoles with *trans*- $\beta$ -Nitrostyrenes<sup>[a]</sup>


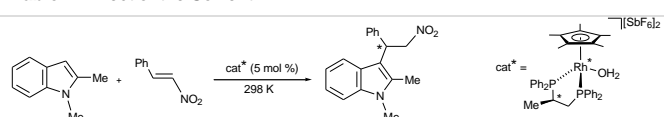
Entry	Cat*	R <sup>1</sup>	R <sup>2</sup>	R <sup>3</sup>	Conv. (%) <sup>[b]</sup>	ee (%) <sup>[c]</sup>	Product
1	1	H	H	H	100	Rac.	3a
2	2	H	H	H	47	6	3a
3	1	H	H	2-OMe	98	16	3b
4	2	H	H	2-OMe	94	32	3b
5	1	H	H	2-Cl	97	35	3d
6	2	H	H	2-Cl	90	26	3d
7	1	4-OMe	H	H	100	16	3g
8	2	4-OMe	H	H	86	17	3g
9	1	5-I	H	H	80	4	3i
10	2	5-I	H	H	78	5	3i
11	1	Me	H	H	100	14	3k
12	2	Me	H	H	62	18	3k
13	1	Me	H	4-OMe	100	23	3l
14	2	Me	H	4-OMe	90	6	3l
15	1	Me	H	2,3-(OMe) <sub>2</sub>	29	-74	3m
16	2	Me	H	2,3-(OMe) <sub>2</sub>	57	+73	3m
17	1	Me	H	4-Cl	100	+16	3o
18	2	Me	H	4-Cl	55	-22	3o
19	1	H	Me	H	100	+10	3p
20	2	H	Me	H	100	-5	3p
21	1	H	Me	2-OMe	100	14	3q
22	2	H	Me	2-OMe	93	6	3q
23	1	H	Me	2-Cl	100	14	3s
24	2	H	Me	2-Cl	99	3	3s
25	1	H	Me	2,3-(OMe) <sub>2</sub>	100	95	3t
26	2	H	Me	2,3-(OMe) <sub>2</sub>	53	90	3t
27 <sup>[d]</sup>	1	Me	Me	H	100	+98	3u
28	2	Me	Me	H	58	-35	3u

29	1	Me	Me	2-OMe	100	+90	3v
30 <sup>[e]</sup>	2	Me	Me	2-OMe	69	-21	3v
31	1	Me	Me	4-OMe	100	+70	3w
32 <sup>[f]</sup>	2	Me	Me	4-OMe	50	-48	3w
33 <sup>[g]</sup>	1	Me	Me	2-Cl	100	77	3x
34 <sup>[h]</sup>	2	Me	Me	2-Cl	trace	-	3x
35	1	Me	Me	2,3-(OMe) <sub>2</sub>	29	74	3z
36 <sup>[h]</sup>	2	Me	Me	2,3-(OMe) <sub>2</sub>	11	75	3z
37 <sup>[i]</sup>	1	Me	Me	4-Cl	100	90	3ag
38 <sup>[j]</sup>	1	Me	Me	4-Br	100	45	3ah

[a] Reaction conditions: catalyst 0.03 mmol (5.0 mol %), *trans*- $\beta$ -nitrostyrene 0.90 mmol, indole 0.60 mmol and 100 mg of 4 Å molecular sieves, in 4 mL of CH<sub>2</sub>Cl<sub>2</sub>. [b] Based on indole. [c] Determined by <sup>1</sup>H NMR. [d] Determined by HPLC. Reaction time: [d] 5, [e] 210, [f] 150, [g] 90, [h] 300, [i] 15, [j] 10 min

**Scheme 3.** Determination of the Absolute Configuration of 3u**Effect of the solvent**

The model reaction was carried out in a variety of solvents, the remaining reaction conditions being maintained unchanged (Table 2). Coordinating solvents (entries 1-5) slow down the reaction most probably due to competition of the solvent and the substrate for the Lewis acid site of the catalyst. Chlorinated

**Table 2.** Effect of the Solvent<sup>[a]</sup>


Entry	Solvent	t (h)	Conv. (%)	ee (%)
1	CH <sub>3</sub> CN	4	23	rac
2	THF	2	12	15
3	CH <sub>3</sub> COCH <sub>3</sub>	4	70	28
4	CH <sub>3</sub> OH	5	89	5
5	H <sub>2</sub> O	2	100	40
6	CH <sub>2</sub> ClCH <sub>2</sub> Cl	1	100	88
7	CHCl <sub>3</sub>	2.5	76	6
8	CH <sub>2</sub> Cl <sub>2</sub>	0.1	100	98

[a] For reaction conditions, see footnote in Table 1

solvents, different from dichloromethane, also slow down the reaction. In this respect, the formation of small amounts of the catalytically inert chlorinated cation<sup>[23]</sup>  $[(\eta^5\text{-C}_5\text{Me}_5)\text{RhCl}\{(R)\text{-Prophos}}\}]^+$  from the aquo-complex **1** was observed in both 1,2-dichloroethane and chloroform, but not in dichloromethane. Therefore, the decrease in the concentration of active species in the two former solvents would explain the observed deceleration of the catalysis.

The enantiomeric excess varies with the solvent. The best value (98 % ee) was obtained for dichloromethane. In summary, the best rate and selectivity were achieved in dichloromethane and, therefore, it is the solvent of choice.

### Effect of catalyst loading

We next examined the effect of the catalyst loading on the enantioselectivity. Table 3 collects the ee values measured at different catalyst loadings, after quantitative conversion at 283 K. Notably, increasing the catalyst loading above 10 mol % produces an important decrease in the enantiomeric excess and eventually, the catalytic stoichiometric reaction renders racemic adduct (entry 9). These results are unexpected because usually, increasing the catalyst loading either does not alter the stereoselectivity (higher concentration of active species but the same selectivity) or increases the ee (greater catalyzed reaction/thermic reaction ratio). We will turn back to this point later on.

**Table 3.** Effect of Catalyst Loading<sup>[a,b]</sup>

Entry	Cat <sup>†</sup> (mol %)	ee (%)
1	1	98 (S)
2	2	97 (S)
3	5	99 (S)
4	10	94 (S)
5	20	70 (S)
6	30	42 (S)
7	40	36 (S)
8	50	8 (S)
9	100	rac

[a] For reaction conditions, see footnote in Table 1. [b] For reaction model see Table 2

### Effect of the temperature

The model reaction was performed at temperatures over the range 313–233 K, the remaining conditions being maintained unchanged. Table 4 gathers the ee obtained values. Catalytic runs were quenched when the presence of indole (limitant reagent) was not detected in the reaction medium by <sup>1</sup>H NMR spectroscopy. Excellent ee (96–99 %) in the S enantiomer was obtained above 263 K. However, by reducing the temperature below this value, as the unique change in the catalytic conditions,

a decrease of enantioselectivity was observed. Of particular interest is the fact that the major enantiomer is switched from the (S)- to the (R)-FC adduct at around 253 K, and thereafter, the ee in the R enantiomer augments as the temperature further

**Table 4.** Effect of the Temperature<sup>[a,b]</sup>

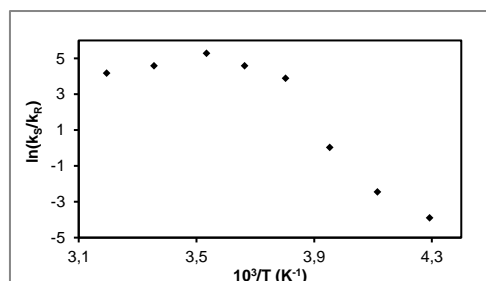
Entry	T (K)	ee (%)
1	313	97 (S)
2	298	98 (S)
3	283	99 (S)
4	273	98 (S)
5	263	96 (S)
6	253	2 (S)
7	243	84 (R)
8	233	96 (R)

[a] For reaction conditions, see footnote in Table 1. [b] For reaction model see Table 2

decreases. Thus, at 243 K, an 84 % ee in the R enantiomer was obtained that increases up to 96 % ee, at 233 K. Therefore, selective access to either (R)- or (S)-FC adducts is possible simply by changing the reaction temperature. As far as we know, such high enantioselection level for both antipodes, achieved by only changing the temperature, has not been reported so far, for catalytic reactions mediated by transition metal complexes.<sup>[3,4]</sup>

The natural logarithms of the relative rate constants affording (R)- and (S)-FC adducts, *i.e.*  $\ln(k_S/k_R)$ , were plotted against the reciprocal of temperature (Figure 1); the  $\ln(k_S/k_R)$  values are calculated according to equation 1, which can also be written as the differential Eyring equation shown in equation 2.<sup>[24]</sup>

If the mechanism of enantioselection is unique over the investigated temperature range,  $\Delta\Delta H^\ddagger$  and  $\Delta\Delta S^\ddagger$  should be constant and therefore a linear plot would be obtained. Conversely, if the enantiodetermining step changes at different temperatures,  $\Delta\Delta H^\ddagger$  and  $\Delta\Delta S^\ddagger$  should vary and the plot would be nonlinear. As the plot importantly deviates from linearity, it can be inferred that the enantiodetermining step is changing over the range of temperature and, most probably, more than one mechanism is operating in the catalytic process.<sup>[3b]</sup>



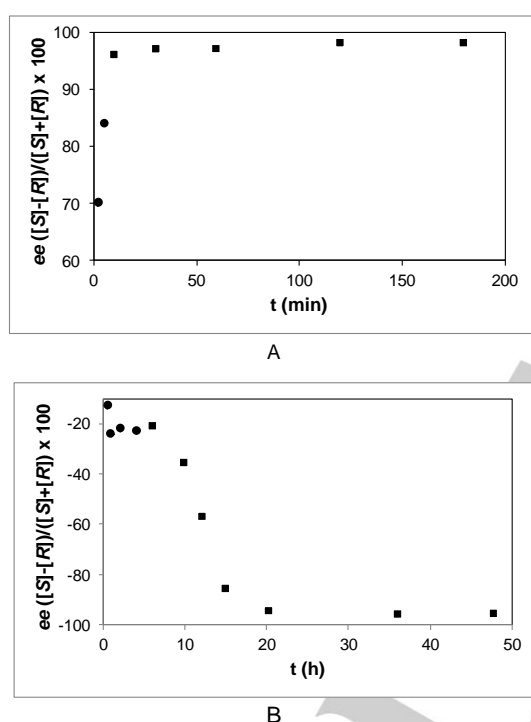
**Figure 1.** Plot of  $\ln(k_S/k_R)$  vs  $1/T$  for the FC process



$$\ln(k_S/k_R) = \ln((100 + \% ee) / (100 - \% ee)) \quad (\text{Eq. 1})$$

$$\ln(k_S/k_R) = -\Delta\Delta H^\ddagger/RT + \Delta\Delta S^\ddagger/R \quad (\text{Eq. 2})$$

It is worth mentioning that at a fixed temperature, the *ee* changes with the reaction time. At temperatures  $\geq 263$  K (for example at 298 K, Figure 2A) concentration of the *S* isomer increases with conversion and the *ee* reached when indole is no longer detected by NMR in the reaction medium remains essentially unaltered at longer reaction times (squares in Figure 2A). Conversely, at temperatures below 253 K (for example at 233 K, Figure 2B) the relative amount of the *S* isomer decreases with conversion, this trend being maintained even after indole is no longer detected in the catalytic solution (squares in Figure 2B). At an intermediate temperature, such as 253 K, low absolute values of *ee* around zero were measured along the reaction time.<sup>[25]</sup>



**Figure 2.** Evolution of the *ee* as  $([S]-[R])/([S]+[R]) \times 100$  versus reaction time when the reaction was carried out at 298 K (A) or at 233 K (B)

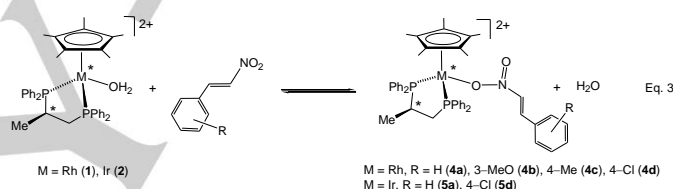
All these experimental data have enabled us to substantiate an unusual temperature dependent reversal in enantioselectivity. The same catalyst can provide either enantiomer as the dominant product with excellent optical purity simply by changing the reaction temperature. Furthermore, significant evidences of the existence of competitive, enantiomerically divergent mechanistic paths are revealed. As a consequence, three main questions arise: i) which is the origin of such a dramatic change in the enantioselectivity by simply changing temperature?; ii) why does the *ee* vary over the reaction time and with dissimilar trends at different temperatures?; iii) why does the *ee* decrease when

catalyst loading increases? Trying to answer these questions, we started studying the catalytic process by NMR spectroscopy.

### The $(S_M, R_C)-[(\eta^5-C_5Me_5)M\{(R)-Prophos\}(H_2O)]^{2+}/trans-\beta$ -nitrostyrenes system

The first step of the reaction would be the coordination of the nucleophile to the metallic catalytic precursor giving rise to the true catalyst. We have therefore studied by NMR spectroscopy the solution behavior of mixtures of complexes **1** or **2** with *trans*- $\beta$ -nitrostyrenes.

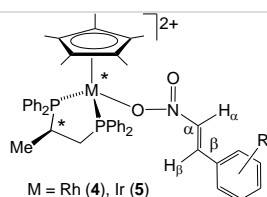
When, at 248 K, 30 equivalents of *trans*- $\beta$ -nitrostyrene were added to a solution of  $(S_{Rh}, R_C)-[(\eta^5-C_5Me_5)Rh\{(R)-Prophos\}(H_2O)]^{2+}$  (**1**) in  $CD_2Cl_2$ ,<sup>26</sup> the new complex  $[(\eta^5-C_5Me_5)Rh\{(R)-Prophos\}(trans-\beta\text{-nitrostyrene})]^{2+}$  (**4a**) was formed according to <sup>31</sup>P NMR measurements. At this temperature, the aquo and nitroalkene complexes are in equilibrium in *ca.* 92/8 molar ratio, the first percentage corresponding to the water complex (Eq. 3). However, in the presence of 4Å molecular sieves, the equilibrium is completely shifted to the right, the nitroalkene complex **4a** being the sole phosphorus containing compound detected in the solution.



Other nitroalkenes such as *trans*-3-methoxy- $\beta$ -nitrostyrene, *trans*-4-methyl- $\beta$ -nitrostyrene and *trans*-4-chloro- $\beta$ -nitrostyrene behave similarly. The homologue iridium compound  $(S_{Ir}, R_C)-[(\eta^5-C_5Me_5)Ir\{(R)-Prophos\}(H_2O)][SbF_6]_2$  (**2**) reacts likewise with nitroalkenes affording the nitroalkene complexes **5a** and **5d** (Eq. 3).

From 298 to 193 K, the NMR spectra in  $CD_2Cl_2$  of the new compounds only show one set of signals indicating that only one stereoisomer is present in the solution. Therefore, the substitution reaction is completely diastereoselective.

The <sup>31</sup>P NMR spectra of the rhodium complexes **4** in  $CD_2Cl_2$  consist of two doublets of doublets centered at about 75.8 and 51.5 ppm, with <sup>1</sup>J(Rh,P) and <sup>2</sup>J(P,P) coupling constants of around 130 Hz and 38 Hz, respectively. The iridium complexes **5** show two doublets at *ca.* 49 and 28 ppm, with a <sup>2</sup>J(P,P) coupling constant of around 10 Hz. Table 5 collects the <sup>1</sup>H and <sup>13</sup>C NMR data for the  $\alpha$  and  $\beta$  protons and carbons of the coordinated nitroalkenes along with the  $\Delta\delta$  undergone by coordination. Notably, a strong shielding (about 1 ppm for the rhodium complexes and about 0.8 ppm for the iridium ones) was observed for the  $H_\beta$  proton. We will come back to this point when discussing the crystal structure of complex **4d**. Conversely, a deshielding of the  $\beta$  carbon (about 7.5 ppm for the rhodium complexes and about 9 ppm for the iridium ones) was detected. This strong deshielding indicates that the  $\beta$  carbon undergoes an important electronic activation towards the nucleophilic attack, when the nitroalkene coordinates to dicationic  $(\eta^5-C_5Me_5)M\{(R)-Prophos\}$  moieties.

**Table 5.** Selected  $^1\text{H}$  y  $^{13}\text{C}$  NMR Data for the Nitroalkene Complexes **4** and **5**<sup>[a]</sup> **$^1\text{H}$  NMR**

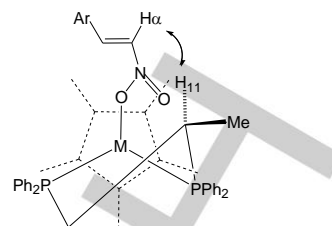
Comple x	R	$\delta\text{H}_\alpha$	$\Delta\delta\text{H}_\alpha$	$\delta\text{H}_\beta$	$\Delta\delta\text{H}_\beta$
<b>4a</b>	H	7.1 8	-0.41	6.99	-1.02
<b>4b</b>	3-OMe	7.1 9	-0.26	6.89	-1.06
<b>4c</b>	4-Me	7.1 7	-0.38	6.95	-1.02
<b>4d</b>	4-Cl	7.1 6	-0.39	6.94	-1.01
<b>5a</b>	H	7.2 6	-0.33	7.15	-0.86
<b>5d</b>	4-Cl	7.2 3	-0.32	7.16	-0.79

 **$^{13}\text{C}$  NMR**

Complex	R	$\delta\text{C}_\alpha$	$\Delta\delta\text{C}_\alpha$	$\delta\text{C}_\beta$	$\Delta\delta\text{C}_\beta$
<b>4a</b>	H	134.21	-2.9 9	146.97	+7.75
<b>4b</b>	3-OMe	134.27	-3.1 9	146.93	+7.76
<b>4c</b>	4-Me	134.20	-2.2 4	147.41	+7.10
<b>4d</b>	4-Cl	134.57	-2.9 8	145.46	+7.66
<b>5a</b>	H	134.40	-2.8 0	148.23	+9.01
<b>5d</b>	4-Cl	132.34	-5.2 1	146.65	+8.85

[a] Chemical shifts in ppm and coupling constants in Hz

In all cases,  $^1\text{H}$ - $^1\text{H}$  NOESY measurements show a NOE correlation between the  $\text{H}_\alpha$  nitroalkene and the  $\text{H}_{11}$  Prophos protons (Scheme 4). This correlation only can take place in diastereomers with *S* configuration at the metal. Therefore, the diastereoselective substitution reaction occurs with retention of the configuration at the metal.

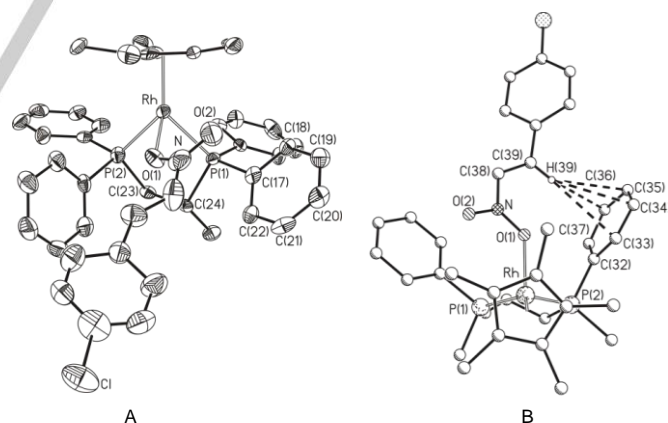
**Scheme 4.** NOE relationship between the  $\text{H}_\alpha$  and  $\text{H}_{11}$  protons

All attempts to isolate pure samples of the nitroalkene complexes **4** and **5** were unsuccessful. From the reaction media, solids containing 5-10 % of the starting aquo-complexes **1** or **2** were isolated. We have not been able to purify them, either by chromatography or by recrystallization. However, single crystals of the rhodium compound **4d**, suitable for X-ray diffraction analysis, were obtained from dichloromethane solutions containing **1** and excess of *trans*-4-chloro- $\beta$ -nitrostyrene.

**Molecular structure of the complex 4d**

A molecular representation of the cation of the complex is shown in Figure 3A. Selected bond lengths and angles are summarized in Table 6. The cation is formally pseudo-tetrahedral with metal coordination to the  $\text{C}_5\text{Me}_5$  ring, to the two phosphorus atoms of the chelate Prophos ligand and to one of the two oxygen atoms of the nitroalkene.

According to the ligand priority sequence,<sup>[27]</sup> the absolute configuration at the metal is *S*. The five-membered metallacycle Rh-P(2)-C(23)-C(24)-P(1) adopts a  $\lambda$  conformation. Cremer and Pople ring puckering parameters ( $Q = 0.481(9)$  Å and  $\phi = 75.8(6)^\circ$ ) are characteristic of a  $^3\text{E}$  conformation.<sup>[28]</sup> The

**Figure 3.** (A) Molecular structure of the cation of **4d**. Hydrogen atoms have been omitted for clarity. (B) Intramolecular CH/ $\pi$  interactions**Table 6.** Selected Bond Distances (Å) and Angles (deg) for the Nitroalkene Complex **4d**

Rh-P(1)	2.342(3)	N-C(38)	1.381(15)
---------	----------	---------	-----------

Rh–P(2)	2.348(4)	P(1)–Rh–P(2)	83.93(7)
Rh–O(1)	2.182(5)	P(1)–Rh–O(1)	83.90(2)
Ir–G <sup>a</sup>	1.865(5)	P(1)–Rh–G <sup>a</sup>	132.84(18)
O(1)–N	1.276(12)	P(2)–Rh–O(1)	83.30(2)
C(38)–C(39)	1.302(17)	P(2)–Rh–G <sup>a</sup>	129.94(18)
C(39)–C(40)	1.498(14)	O(1)–Rh–G <sup>a</sup>	125.80(2)

<sup>a</sup> G represents the centroid of the η<sup>5</sup>-C<sub>5</sub>Me<sub>5</sub> ligand

**Table 7.** Selected Structural Parameters (Å) Concerning CH/π Interactions for Complex **4d**<sup>[a]</sup>

H···Ct	H···Ph (plane)	C–H···C
		C(35): 2.906(12)
		C(36): 2.904(11)
2.666(11)	2.653(11)	C(33): 3.030(10)
		C(34): 2.960(11)

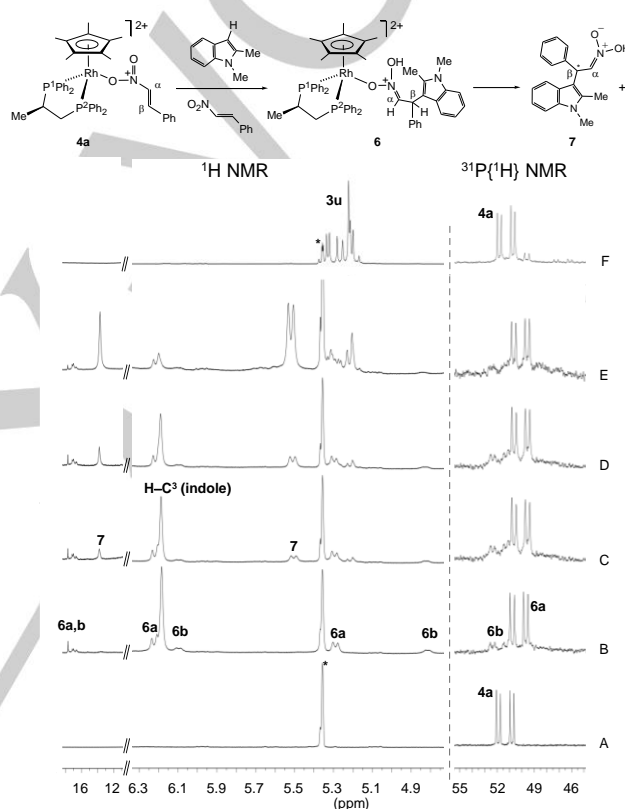
[a] H···Ct represents the distance from the H(39) atom to the centroid of the phenyl ring Ct; H···Ph is the separation from the H(39) atom to the mean plane of the phenyl ring; C–H···C: contact distances between the H(39) atom and phenyl carbon atoms (< 3.05 Å)

nitroalkene ligand coordinates with an *s-trans* conformation and its disposition into the (C<sub>5</sub>Me<sub>5</sub>)Rh{(R)-Prophos} chiral pocket is suitable for the establishment of intramolecular CH/π interactions involving the nitroalkene H<sub>β</sub> proton (H(39) in Fig. 3B) and the *pro-R* phenyl ring C(32)–C(37) of the P(2)Ph<sub>2</sub> group. These interactions are characterized by short H···phenyl-centroid and H···phenyl-plane distances (2.666(11) and 2.653(11) Å, respectively) and by some H···C(phenyl) interatomic distances shorter than the sum of the Van der Waals radii (3.05 Å) (Table 7).<sup>[29]</sup> These interactions place the nitroalkene H<sub>β</sub> proton inside of the electronic diamagnetic ring current of the phenyl ring of the P(2)Ph<sub>2</sub> group (Figure 3B). Most probably, they are also operating in solution giving rise to the strong shielding observed for the H<sub>β</sub> proton.

### The (S<sub>Rh</sub>, R<sub>C</sub>)-[(η<sup>5</sup>-C<sub>5</sub>Me<sub>5</sub>)Rh{(R)-Prophos}(*trans*-β-nitrostyrene)]<sup>2+</sup>/*N*-methyl-2-methylindole system

After coordination of the nitroalkene, the next step of the catalytic cycle would be the reaction of the nitroalkene complex with indole. To confirm this proposal, the reaction of **4a**, formed *in situ* from (S<sub>Rh</sub>, R<sub>C</sub>)-[(η<sup>5</sup>-C<sub>5</sub>Me<sub>5</sub>)Rh{(R)-Prophos}(H<sub>2</sub>O)][SbF<sub>6</sub>]<sub>2</sub> (1, 1 equivalent) and *trans*-β-nitrostyrene (10 equivalents), with *N*-methyl-2-methylindole (5 equivalents) was monitored by NMR spectroscopy. Selected regions of the <sup>1</sup>H and <sup>31</sup>P NMR spectra in CD<sub>2</sub>Cl<sub>2</sub> are depicted in Figure 4. Trace A shows the spectra, at 193 K, of the nitroalkene complex **4a** in these regions: the proton NMR spectrum is silent and a doublet of doublets assigned to the P<sup>2</sup> phosphorus nucleus, appears in the selected zone of the <sup>31</sup>P NMR spectrum.

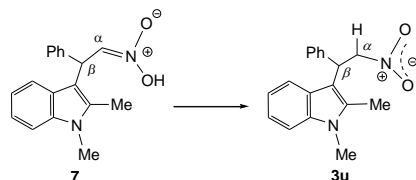
After the addition of the indole, the immediate disappearance of **4a** with concomitant formation of two diastereomers of the rhodium *aci*-nitro complex **6**, in ca. 70 to 30 molar ratio, was observed. The <sup>1</sup>H NMR spectrum of **6** at 193 K (trace B) shows two pairs of coupled doublets centered at 6.22 (H<sub>α</sub>) and 5.29 (H<sub>β</sub>) ppm (major isomer) and at 6.10 (H<sub>α</sub>) and 4.81 (H<sub>β</sub>) ppm (minor) together with an unresolved deshielded resonance at about 17.5 ppm tentatively attributed to the OH functionality. Correspondingly, the <sup>31</sup>P NMR spectrum shows two new doublets of doublets (one much less abundant) attributed to the P<sup>2</sup> nucleus of two isomers of **6**.<sup>[30]</sup>



**Figure 4.** Trace A: Selected regions of the <sup>1</sup>H and <sup>31</sup>P NMR spectra of **4a**, at 193 K. Trace B: Measured at 193 K after the addition of *trans*-β-nitrostyrene and *N*-methyl-2-methylindole in 1/10/5 catalyst/nitroalkene/indole molar ratio. Traces C–E: Measured at 193 K after heating up to 223 K for 20 min. Trace F: Measured at 193 K after total consumption of the indole. Asterisk denotes residual not deuterated dichloromethane

At 193 K, the NMR spectra of trace B do not change for hours. However, when the solution was heated up to 223 K, the successive <sup>1</sup>H NMR spectra recorded at 193 K<sup>[31]</sup> (traces C–E) showed the gradual consumption of the indole (C<sup>3</sup>-H resonance at 6.20 ppm) with the concomitant appearance of a new organic compound (doublet at 5.51 (H<sub>β</sub>) and singlet at 14.12 (OH) ppm) that was spectroscopically identified<sup>[30]</sup> as the *aci*-nitro compound **7** (see equation in Figure 4).

Further treatment at 223 K gave rise to the progressive formation of the FC adduct **3u** at the expense of **7** (trace F) through the prototropic tautomerism depicted in Scheme 5. Simultaneously, the remaining *trans*- $\beta$ -nitrostyrene displaced the *aci*-nitro ligand in **6** regenerating the nitroalkene complex **4a**.



Scheme 5. Prototropic tautomerism

### The catalytic path

Based on the sequential steps discussed above, the catalytic cycle **A**, depicted in Figure 5, could be proposed. The coordinated water molecule in **1** is displaced by *trans*- $\beta$ -nitrostyrene, giving the nitroalkene complex **4a**. Indole attack to the activated C $\beta$  of the coordinated nitroalkene renders the *aci*-nitro complexes **6**. Reaction of **6** with a new molecule of *trans*- $\beta$ -nitrostyrene eliminates the *aci*-nitro ligand **7** and regenerates complex **4a** that restarts the cycle. Finally, free *aci*-nitro **7** rearranges to the FC adduct **3u**.

Cycle **A** rationalizes the formation of the FC adduct and accounts for a pathway involving the detected intermediates **4a**, **6a,b** and **7**. However, this cycle does not answer any of the above aroused questions. Indeed, as a 70/30 diastereomeric ratio was measured for complexes **6**, *ee* values of only around 40 % would be expected. To account for the high *ee* values obtained, we envisaged the possibility that a dynamic kinetic resolution (DKR) would take place on **6** *i. e.* one of the *aci*-nitro enantiomers is preferentially dissociated from **6** and cycle **A** was reversible. Hence, we will continue studying the reversibility of this cycle.

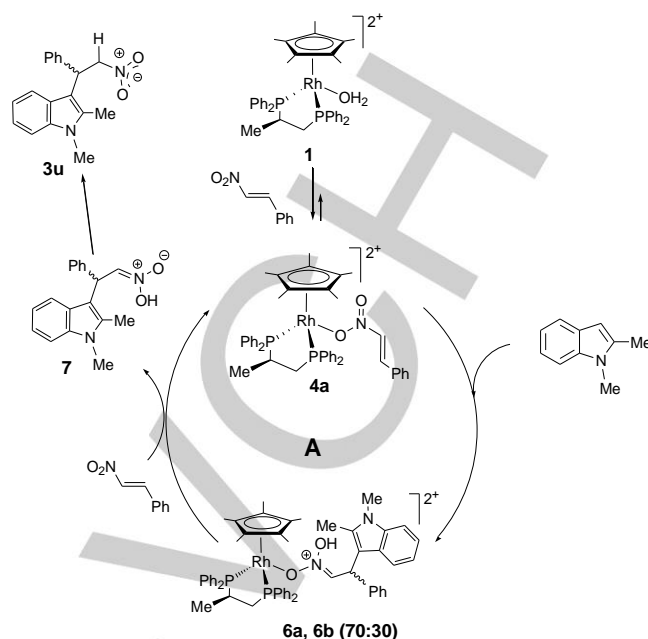


Figure 5. Catalytic cycle **A**

### Reversibility of the cycle **A**

To assess the reversibility of the cycle **A**, a solution containing **6** and **7** was prepared by mixing **1**, *trans*- $\beta$ -nitrostyrene and *N*-methyl-2-methylindole, in 1/25/20 molar ratio, in CD<sub>2</sub>Cl<sub>2</sub> and allowing the mixture to react, at 233 K, until the indole was not observed in the <sup>1</sup>H NMR spectrum (see SI). Trace A in Figure 6 displays the 6.4–5.0 ppm region of this spectrum recorded at 233 K. In this zone, the spectrum presents a doublet centered at 5.58 ppm, attributed to the H $\beta$  proton of the *aci*-nitro compound

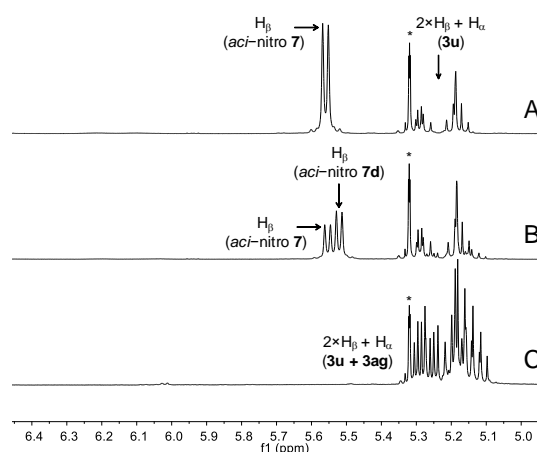
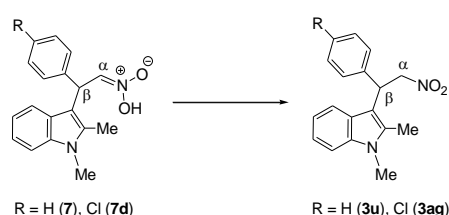


Figure 6. Selected region of the <sup>1</sup>H NMR spectrum of a 1/*trans*- $\beta$ -nitrostyrene/*N*-methyl-2-methylindole, 1/25/20 molar ratio mixture allowed to react, at 233 K, until the indole was not observed in the spectrum (trace A). After the addition of *trans*-4-chloro- $\beta$ -nitrostyrene (trace B). After warming up to 298 K (trace C)

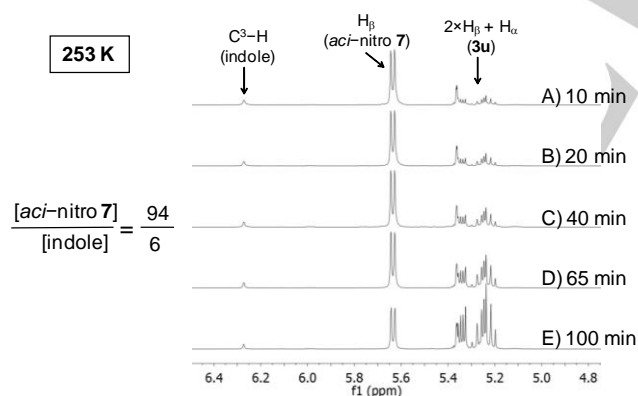


**7** along with complex signals around 5.2 ppm, due to the  $H_{\alpha}$  and  $H_{\beta}$  protons of a small amount of the FC adduct **3u**. Although, at 233 K, the  $H_{\alpha}$  and  $H_{\beta}$  protons of complexes **6** are not observed in the  $^1\text{H}$  NMR spectrum, the  $^{31}\text{P}$  NMR spectrum (not shown) clearly establish the presence of these compounds. Maintaining the temperature at 233 K, *trans*-4-chloro- $\beta$ -nitrostyrene was added in 1/1 molar ratio with respect to the previously added *trans*- $\beta$ -nitrostyrene. The  $^1\text{H}$  NMR spectrum (trace B) reveals the immediate appearance of a new doublet centered at 5.52 ppm that we assign to the corresponding *aci*-nitro compound **7d** derived from *N*-methyl-2-methylindole and *trans*-4-chloro- $\beta$ -nitrostyrene. When temperature was raised up to 298 K, the **7** and **7d** doublets disappeared and complex signals in the 5.1-5.35 ppm region were observed (trace C). These resonances were attributed to a mixture of the FC compounds **3u** and **3ag** (Scheme 6) by HPLC analysis.

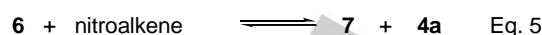
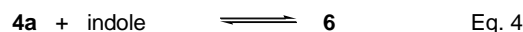


**Scheme 6.** *Aci*-nitro (**7**) and Friedel-Crafts (**3**) compounds

According to  $^1\text{H}$  NMR data, when the chlorinated nitroalkene was added, the amount of indole was negligible. The source of indole required for the generation of **3ag** must be compound **7**; thus observation of **3ag** in this experiment proves that reactions  $4a + \text{indole} \rightleftharpoons 6$  and  $6 + \text{nitroalkene} \rightleftharpoons 4a + 7$  (Figure 5) are reversible to some extent.



**Figure 7.** Evolution of the  $^1\text{H}$  NMR spectra of a mixture of **1**, *trans*- $\beta$ -nitrostyrene and *N*-methyl-2-methylindole in 1/30/20 molar ratio, in  $\text{CD}_2\text{Cl}_2$ , at 253 K



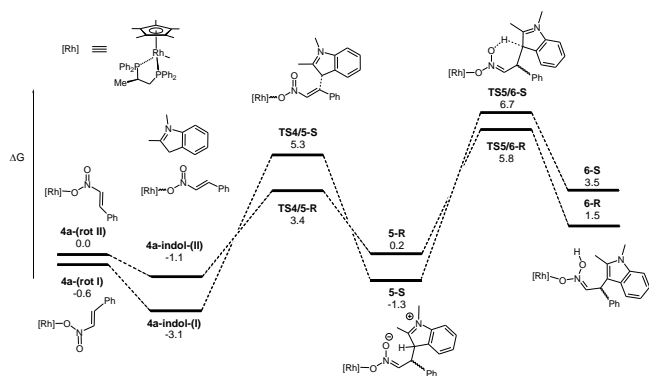
On the other hand, in independent experiments, two identical solutions were prepared by mixing **1**, *trans*- $\beta$ -nitrostyrene and *N*-methyl-2-methylindole in 1/30/20 molar ratio in  $\text{CD}_2\text{Cl}_2$ . The course of the catalytic reaction was monitored by NMR at 273 K for one solution and at 253 K for the other. Figure 7 collects the spectra recorded at 253 K. Those recorded at 273 K are depicted in Figure S3 (SI). As shown in Figure 7, the amount of the FC product **3u** was increasing with reaction time but the *aci*-nitro(**7**)/indole ratio remained constant with a value of 96/4. Furthermore,  $^1\text{H}$ - $^1\text{H}$  EXSY cross-peaks reveal the exchange of the indole  $\text{C}^3$ -H proton with the OH proton of the *aci*-nitro compound (see SI). This behavior can again be explained by assuming that the observed equilibrium between indole and *aci*-nitro compound **7** (Eq. 6) is the sum of the above mentioned equilibria between **4a** and **6** (Eq. 4) and between **6** and **7** + **4a** (Eq. 5).

In summary, all these experimental data strongly indicated that both the reaction of the coordinated nitroalkene with indole (step  $4a \rightleftharpoons 6a,b$ ) and the exchange of the *aci*-nitro compounds by nitroalkene (step  $6a,b \rightleftharpoons 4a$ ) are reversible, *i.e.* cycle **A** is reversible.

#### Theoretical calculations for the step $4a + \text{indole} \rightleftharpoons 6$

Looking for a better understanding of the catalytic results, DFT calculations at the B3LYP-D3/def2-SVP level were carried out (see Experimental Section for computational details). The calculated free-energy profile of the step  $4a + \text{indole} \rightleftharpoons 6$  is shown in Figure 8.

The *trans*- $\beta$ -nitrostyrene molecule may coordinate the metal adopting two different conformations: **4a**-(rot II) and **4a**-(rot I), being the latter slightly more stable than the former (0.6 kcal/mol). Both conformers are interchangeable by rotation along the Rh-O single bond. Then, in solution, they are involved in a quick equilibrium and sharp weighted average signals were observed in the NMR spectra. Due to the spatial disposition of the (*R*)-Prophos ligand, the *N*-methyl-2-methylindole can only approach the *trans*- $\beta$ -nitrostyrene by the *Re*-face in **4a**-indol-(II) and by the *Si*-face in **4a**-indol-(I), rendering *R* and *S* at  $\text{C}_{\beta}$  derivatives, respectively.



**Figure 8.** Reaction profiles and relative Gibbs free energies (kcal/mol) for the reactions of cycle **A**, computed at the DFT level and PCM solvent ( $\text{CH}_2\text{Cl}_2$ ) corrections, at 298.15 K

Figure 8 shows the two possible diastereo-related pathways of the considered step. The formation of the C–C bond and proton transfer to the uncoordinated oxygen atom of the nitro group take place in a stepwise manner via the intermediates **5-R** and **5-S**. The transition structures for the nucleophilic attack of the *N*-methyl-2-methylindole carbon atom to the *trans*- $\beta$ -nitrostyrene, **TS4/5-R** and **TS4/5-S**, present relative energies of 3.4 and 5.3 kcal/mol, respectively. The zwitterionic intermediates **5-R** and **5-S** show relative energies of 0.2 and –1.3 kcal/mol while the second transition structures **TS5/6-R** and **TS5/6-S**, corresponding to the proton transfer and formation of the *aci*-nitro compound, present relative free energies of 5.8 and 6.7 kcal/mol. The obtained *aci*-nitro compounds, **6-R** and **6-S**, show relative energies of 1.5 and 3.5 kcal/mol. These energetic values indicate that both processes are accessible and reversible under the experimental conditions employed, in agreement with the experimental data above reported. Noteworthy, the *aci*-nitro complex **6-R** is 2.0 kcal/mol more stable than its homologue **6-S** due to the more favorable interaction with the catalyst. Inspection of the molecular geometries of intermediates **6-R** and **6-S** does not show specific interactions between the coordinated *aci*-nitro moiety and the chiral pocket created by the ligands surrounding the metallic center.

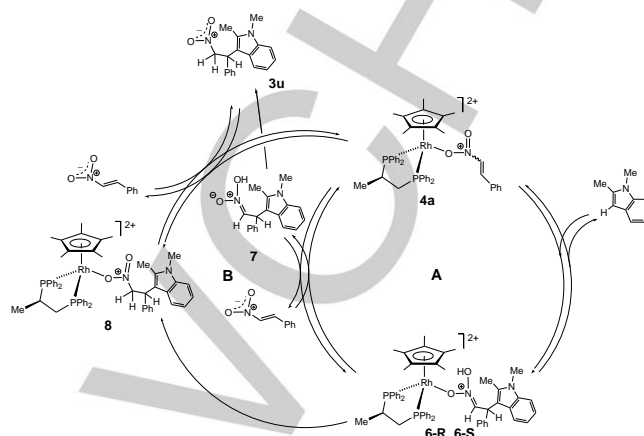
### The 1,3-prototropic tautomerism step

The proposed catalytic process includes the uncatalyzed prototropic tautomerism step **7**  $\rightarrow$  **3u** (see Scheme 5). Taking into account that the experimental data strongly indicate the existence of more than one catalytic mechanism, we envisaged the possibility that the prototropic tautomerism would also occur when the *aci*-nitro compound is coordinated to the metal. Therefore, we postulated a new intermediate in which the FC adduct is coordinated to the metal.

In fact, when, at 193 K, 10 equivalents of racemic **3u** were added to a dichloromethane solution of the aqua-complex ( $S_{\text{Rh}}, R_{\text{C}}$ )- $[(\eta^5\text{-C}_5\text{Me}_5)\text{Rh}\{(\text{R})\text{-Prophos}\}(\text{H}_2\text{O})][\text{SbF}_6]_2$  (**1**), in the presence of molecular sieves, two new doublets of doublets, in the  $^{31}\text{P}$  NMR spectrum, denote the formation of new metallic complexes. We attribute these signals to two diastereomers of the

FC adduct complex  $[(\eta^5\text{-C}_5\text{Me}_5)\text{Rh}\{(\text{R})\text{-Prophos}\}(\mathbf{3u})]^{2+}$  (**8**) (see Experimental Section).

By including species **8**, the alternative catalytic path depicted in Figure 9 (cycle **B**), can be proposed.

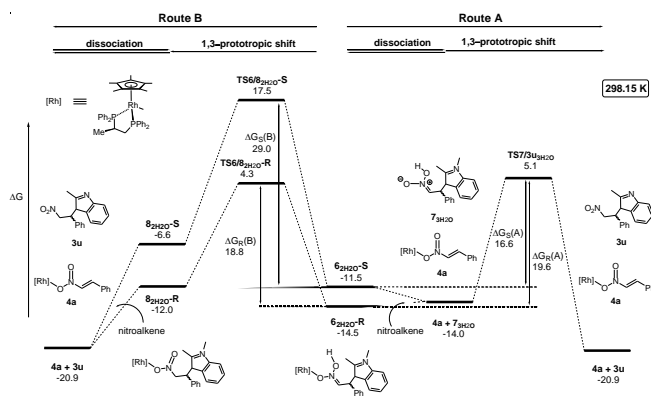


**Figure 9.** Cycles **A** and **B**

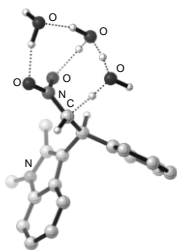
### Theoretical calculations for the 6 to 3u routes

Next, theoretical calculations were carried out for the two routes from **6** to **3u** following, alternatively, cycle **A** (route **A**) or cycle **B** (route **B**). Calculations were performed at 298.15 and 233.15 K, taking into account that carrying out the catalytic reaction at 298 K a 98% ee in the *S* enantiomer was achieved whereas working at 233 K a 96% ee in the *R* isomer was obtained (see Table 4). Activation energies for the 1,3-prototropic tautomerism were found excessively high. However, energetically affordable activation barriers were obtained when water molecules, which can be present in the reaction media, were included explicitly in the calculation according to a Grothius-type mechanism.<sup>[32]</sup>

Figure 10 shows the DFT Gibbs free energy profile for both routes, **A** (from center to right) and **B** (from center to left), at 298.15 K. Following route **A**, the *aci*-nitro compound **7** after dissociation from **6**, isomerizes to the final product **3u** by means of a 1,3-prototropic shift. Three discrete water molecules have been explicitly considered in the DFT calculations for the corresponding transition structure **TS7/3u<sub>3H2O</sub>** (see Figure 11). The obtained energy barriers are 19.6 and 16.6 kcal/mol, for the **6-R** and **6-S** isomers, respectively.



**Figure 10.** Reaction profiles and relative Gibbs free energies (kcal/mol) for the prototropic tautomerism and dissociation steps, computed at the DFT level and PCM solvent ( $\text{CH}_2\text{Cl}_2$ ) corrections, at 298.15 K



**Figure 11.** Grothuss-type mechanism

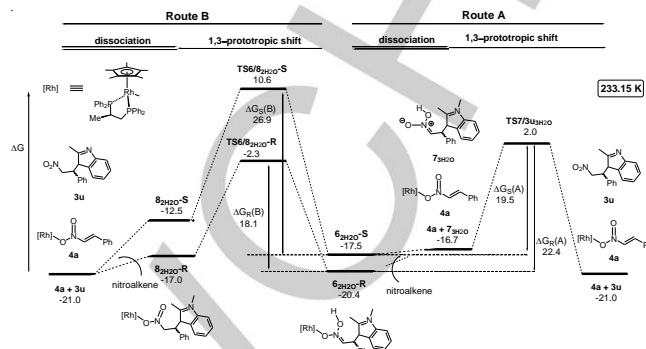
Similarly, in route **B**, the participation of water molecules is necessary for the 1,3-prototropic shift in  $6_{2\text{H}_2\text{O}}\text{-R}$  and  $6_{2\text{H}_2\text{O}}\text{-S}$ .<sup>[33]</sup> Hence, complexes  $6\text{-R}$  and  $6\text{-S}$  may accommodate two water molecules, forming intermediates  $6_{2\text{H}_2\text{O}}\text{-R}$  and  $6_{2\text{H}_2\text{O}}\text{-S}$ , respectively. At 298.15 K, the transition states corresponding to the proton transfer process are  $\text{TS6/8}_{2\text{H}_2\text{O}}\text{-R}$  and  $\text{TS6/8}_{2\text{H}_2\text{O}}\text{-S}$  (activation barriers of 18.8 and 29.0 kcal/mol, for the *R* and *S* enantiomers, respectively) leading to the (*R*)-**3u** and (*S*)-**3u** FC adducts through the corresponding FC adduct coordinated **8**.

Therefore, at 298.15 K, the formation of the *S* enantiomer of the adduct **3u** through route **A** presents the lowest activation barrier ( $\Delta G_{\text{S}}(\text{A}) = 16.6$  kcal/mol) while the formation of the *R* enantiomer ( $\Delta G_{\text{R}}(\text{B}) = 18.8$  kcal/mol) is 2.2 kcal/mol more unfavorable. The uncatalyzed prototropic shift from **7** to **3u** is the rate-determining step of the overall mechanism at 298.15 K.

Figure 12 shows the DFT Gibbs free energy profile for both routes **A** (from center to right) and **B** (from center to left), at 233.15 K. From a similar analysis to that at 298.15 K, it can be concluded that the prototropic shift **6** → **8** is the rate-determining step and that, at 233.15 K, the formation of the *R* enantiomer through route **B** ( $\Delta G_{\text{R}}(\text{B}) = 18.1$  kcal/mol) of the adduct **3u**, presents the lowest activation barrier.

Interestingly, dissociation of the *aci*-nitro compound is more favorable for **6-S** than for **6-R** at all the temperatures considered and with or without water molecules. The **6-R** complex is 1.5–3 kcal/mol more stable than the corresponding **6-S** complex as it

can be seen in Figures 10, 12 and S5. This result, together with the reversibility of cycle **A**, strongly indicates that, at both temperatures, in the step **6** → **7**, the *S* enantiomer is preferentially obtained due to the DKR in **6**.



**Figure 12.** Reaction profiles and relative free energies (kcal/mol) for the prototropic tautomerism and dissociation steps, computed at the DFT level including PCM solvent ( $\text{CH}_2\text{Cl}_2$ ) corrections at 233.15 K

On the other hand, complex **8** is the only new compound detected in dichloromethane solutions containing aqua-complex **1** and FC adduct **3u**. Additionally, we have not detected the formation of the FC chlorinated adduct **3ag** in mixtures of aqua-complex **1**, FC adduct **3u** and *trans*-4-chloro- $\beta$ -nitrostyrene neither over one day at 298 K nor over 3 days at 233 K. These data, together with the high calculated barriers, strongly indicate that the steps **6** → **8** and **7** → **3y** are essentially irreversible.

In summary, the theoretical calculations carried out, together with the experimental data, justify the high values of the *ee* achieved and the stereo-divergence experimentally encountered. At all the investigated temperatures, the *S* enantiomer of the *aci*-nitro compound **7** is formed in high concentration and excellent enantiopurity due to the DKR that occurs in **6**. At high temperature, compound **7** undergoes an uncatalyzed 1,3-prototropic shift rendering the *S* isomer of the FC adduct **3u** in excellent *ee*. At low temperature, the catalyzed 1,3-prototropic shift (step **6** → **8**) is kinetically favored with respect to the uncatalyzed prototropic shift (step **7** → **3u**) and, consequently, the *S* enantiomer of the *aci*-nitro compound **7** evolves to the *R* enantiomer of the FC adduct **3u**, through the *aci*-nitro complexes **6**. This enantiomer is obtained in high purity because the catalyzed prototropy occurs more easily for the *R* ( $\Delta G_{\text{R}}(\text{B}) = 18.1$  kcal/mol) than for the (*S*)- $\text{C}_{\beta}$  diastereomer ( $\Delta G_{\text{S}}(\text{B}) = 26.9$  kcal/mol, Figure 12). Therefore, at low temperature, the DKR in **6** favors the formation of the (*R*)- $\text{C}_{\beta}$  diastereomer of complex **8** which dissociates highly enantioenriched (*R*)-**3u** according to cycle **B**.

Furthermore, on these bases, a plausible explanation for the evolution of the value of the *ee* with the reaction time, at a fixed temperature (Figure 2 and SI), can be proposed. At high temperature (above 253 K), the *ee* in the (*S*)-**3u** FC adduct increases as conversion increases (Figure 2A) because a better DKR in **6** was achieved with longer reaction times until the indole,

the limiting reagent, was consumed. Then, the *ee* becomes constant. However, at low temperature (below 253 K), the *ee* in the (*R*)-**3u** FC adduct increases when reaction time increases, even when no indole is detected in the reaction medium, by NMR spectroscopy (Figure 2B). Below 253 K, the catalytic solution consists of *aci*-nitro compound **7** (mostly the *S* isomer) and metallic complexes **6**. The product **3u** is slowly formed, mainly as the *R* isomer, from the *aci*-nitro compound **7** through the route **7** → **6**, **6** ⇌ **4**, **6** → **8** → **3u**, in which, a DKR takes place in **6**, in favor of the *R* at *C*<sub>β</sub> diastereomer. At short reaction times, formation of **3u** from **7** by this route is not complete and the remaining **7** generates (*S*)-**3u** after quenching the catalytic reaction,<sup>[34]</sup> with the concomitant decrease of the *ee* in the *R* isomer. At longer reaction times the conversion of **7** in (*R*)-**3u** through **6** and **8** increases with the subsequent increment in the concentration of the *R* isomer with time.

### Kinetic studies for the step **6** → **8**

According to experimental and theoretical data, at 233 K, the uncatalyzed tautomeric prototropy, **7** → **3u**, is precluded and the FC adduct **3u** is mostly obtained through the route **7** → **6** → **8** → **3u** (Figure 13). In this route, the catalyzed prototropic tautomerism, **6** → **8**, is the rate-determining step and, therefore, kinetic data can be experimentally obtained for this step by monitoring the transformation of **7** into **3u**.

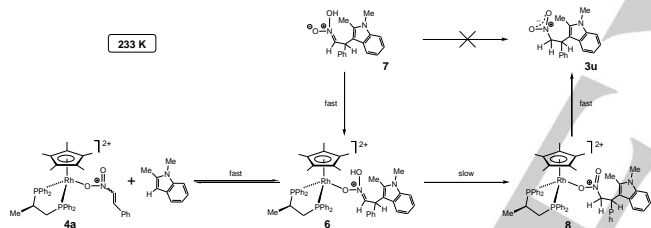


Figure 13. Reaction pathway from **7** to **3u**, at 233 K

To this end, a dichloromethane solution containing **7** and **6** was prepared from **1**, *trans*- $\beta$ -nitrostyrene and *N*-methyl-2-methylindole, as indicated above. The concentration of *aci*-nitro **7** versus time at catalyst loadings ranging from 7 to 17 mol %, at 233 K, is plotted in Figure 14.

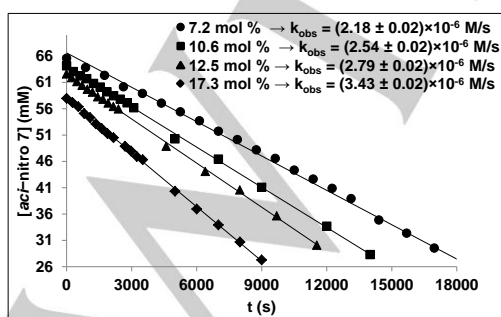


Figure 14. Plot of the concentration of **7** versus time, at 233 K, at different catalyst loadings

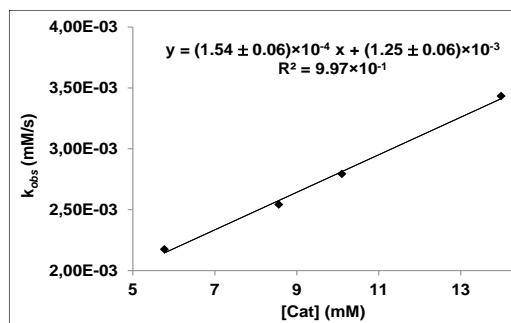


Figure 15.  $k_{obs}$  versus catalyst concentration

The linear dependence indicates that the reaction is of zero order with respect to the *aci*-nitro compound **7**. Furthermore, the observed rate constants show a linear dependence on the concentration of the catalyst, indicating that the reaction is of first order with respect to the catalyst (Figure 15).

Finally, from the Eyring equation a value of 17.5 kcal/mol was obtained for the  $\Delta G^\ddagger$  at 233 K, in good agreement with the calculated  $\Delta G^\ddagger$  at 233.15 K for the step **6** → **8** (18.1 kcal/mol, Figure 12).

### Effect of catalyst loading

According to the obtained kinetic data, while increasing the concentration of the catalyst increases the rate of the catalyzed prototropy **6** → **8**, the rate of the uncatalyzed process **7** → **3u** is not affected. Hence, increasing catalyst loading at 233 K, benefits the reaction affording (*R*)-**3u** as FC product, rather than that rendering the (*S*)-**3u** isomer. Thus, increasing the catalyst loading at 233 K would increase the *ee* in favor of the *R* isomer and *vice versa*.

Figure 16 collects the values of the *ee* measured, at 233 K, at different catalyst loadings, for the reaction between *trans*- $\beta$ -nitrostyrene and *N*-methyl-2-methylindole. Each point of Figure 16 was obtained in an independent experiment. Reaction times were prolonged until at least three constant values of *ee* were measured for each catalyst loading. As expected, *ee* increases from 91.8 % (*R* isomer) up to 99.3 % when catalyst loading increases from 1 to 15 mol %.

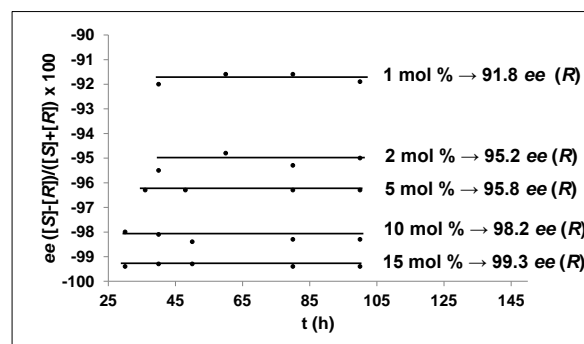


Figure 16. Plot of *ee* as a function of catalyst loading, at 233 K



At 283 K, the FC adduct (*S*)-**3u** is mostly formed through the uncatalyzed prototropy **7** → **3u**. Thus, increasing the catalyst loading increases the fraction of (*R*)-**3u** formed through the catalyzed prototropy **6** → **8** and, therefore, the *ee* in the (*S*)-**3u** isomer would decrease. Indeed, *ee* decreases from 98.5 % (*S* isomer) to 80.0 % when catalyst loading increases from 5 to 15 mol % (Figure 17).

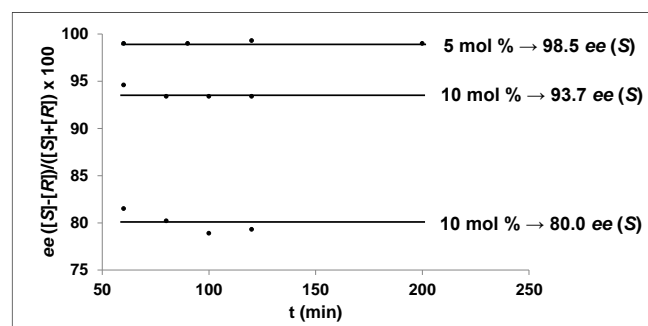


Figure 17. Evolution of *ee* with catalyst loading, at 283 K

### Extension to other *trans*- $\beta$ -nitrostyrenes

When indoles different from *N*-methyl-2-methylindole such as the parent indole, *N*-methylindole or 2-methylindole were allowed to react with *trans*- $\beta$ -nitrostyrene, quantitative conversions were achieved in most cases but with poor *ee* (see Tables S1-S7, SI). Temperature changes do not bring about inversion of the enantioselectivity.

On the other hand, both enantiomers of the FC adduct of the reaction between *N*-methyl-2-methylindole and a series of substituted *trans*- $\beta$ -nitrostyrenes can be obtained working at 298 K or 233 K (Table 8). In several cases, high enantioselectivity was achieved for both enantiomers (entries 1-3, 10). Although in some other cases both antipodes were not obtained, the observed trend suggests that below 233 K (entries 4-7, 13, 14) or above 298 K (entries 8, 9, 11, 17, 18), inversion of the *ee* sign could also be occur for these systems.<sup>[35]</sup>

Table 8. Asymmetric FC Alkylation Reactions of *N*-Methyl-2-methylindole with *trans*- $\beta$ -Nitrostyrenes<sup>[a]</sup>

Entry	R	T (K)	<i>ee</i> (%)	Product
1	2-OMe	298/233	+90/-73	<b>3v</b>
2	3-OMe	298/233	+89/-87	<b>3aa</b>
3	4-OMe	298/233	+70/-99	<b>3w</b>
4	4-Me	298/233	+70/+19	<b>3ab</b>
5	2-OBn	298/233	+4/+2	<b>3ac</b>

6	3-OBn	298/233	+78/+25	<b>3ad</b>
7	4-OBn	298/233	+75/+2	<b>3ae</b>
8	2-Cl	298/233	-77/-96	<b>3x</b>
9	3-Cl	298/233	rac/-58	<b>3af</b>
10	4-Cl	298/233	+90/-95	<b>3ag</b>
11	2-Br	298/233	-39/-42	<b>3y</b>
12	4-Br	298/233	+45/-47	<b>3ah</b>
13	2,3-(OMe) <sub>2</sub>	298/233	-74/-51	<b>3z</b>
14	2,4-(OMe) <sub>2</sub>	298/233	+63/+3	<b>3ai</b>
15	2,5-(OMe) <sub>2</sub>	298/233	+21/-15	<b>3aj</b>
16	3,4-(OMe) <sub>2</sub>	298/233	+60/-5	<b>3ak</b>
17	3-OBn, 4-OMe	298/233	+80/+82	<b>3al</b>
18	2,4-Cl <sub>2</sub>	298/233	-27/-69	<b>3am</b>

[a] For reaction conditions, see footnote of Table 1

## Conclusions

In summary, simply by changing reaction temperature, selective access to both enantiomers of FC adducts derived from the reaction between *N*-methyl-2-methylindole and *trans*- $\beta$ -nitrostyrene is possible by using (*S*<sub>Rh</sub>, *R*<sub>C</sub>)-[( $\eta^5$ -C<sub>5</sub>Me<sub>5</sub>)Rh{(*R*)-Prophos}(H<sub>2</sub>O)][SbF<sub>6</sub>]<sub>2</sub> as catalyst precursor. With selected substituted *trans*- $\beta$ -nitrostyrenes very high enantioselection in both antipodes can be achieved as well. Experimental spectroscopic and kinetic data along with theoretical calculations support the existence of two competitive pathways that essentially differ in the prototropic rearrangement at the *aci*-nitro compound intermediate that can be either rhodium-catalyzed or not. In the *trans*- $\beta$ -nitrostyrene case, at temperatures above 253 K, the catalytic system renders mainly the *S* isomer (96-99 % *ee*) of the FC product through the uncatalyzed prototropic path. At temperatures below 253 K, the catalyzed prototropic path becomes more important and at 233 K the *R* isomer is obtained with 96 % *ee*. A kinetic resolution in favor of the (*S*)-C $\beta$  diastereomer occurs for the dissociation of the *aci*-nitro compound in complexes **6** (step **6** → **7** of cycle **A**) and, conversely, a kinetic resolution in favor of the (*R*)-C $\beta$  diastereomer takes place for the rhodium-catalyzed prototropy (step **6** → **8** of cycle **B**). The reversibility of cycle **A** making dynamic these two kinetic resolutions accounts for the very high *ee* encountered for both enantiomers of the FC product. The evolution of the *ee* over the reaction time and its temperature dependence are also rationalized on the basis of the two proposed catalytic cycles. Finally, kinetic studies support an explanation for the observed uncommon effect of the catalyst loading on the *ee*.

## Experimental Section

### General Information

All manipulations were performed under an inert atmosphere of argon by using Schlenk or NMR tube techniques. Dry, oxygen-free solvents were employed.  $^1\text{H}$ ,  $^{13}\text{C}$  and  $^{31}\text{P}$  NMR spectra were recorded on ARX 300, AV 400 and AV 500 (Bruker) spectrometers.  $^1\text{H}$ , and  $^{13}\text{C}$  NMR chemical shifts are reported in ppm relative to  $\text{SiMe}_4$  as internal standard.  $^{31}\text{P}$  NMR downfield chemical are expressed in ppm relative to 85 %  $\text{H}_3\text{PO}_4$ .  $^1\text{H}$  correlation spectra were obtained using standard procedures. Flash chromatography was performed with a Puriflash 450 (Interchim) chromatograph. Analytical high performance liquid chromatography (HPLC) was performed on an Alliance Waters (Water 2996 PDA detector) instrument using chiral columns Chiralpak IA, IB, IC, OD-H and AD-H (0.46 cm  $\times$  25 cm). Mass spectra were obtained with a Micro Tof-Q Bruker Daltonics spectrometer. Optical rotation was recorded on a Perkin-Elmer-241 polarimeter (10 cm cell, 589 nm).

### Catalytic procedure

Under argon, to a Schlenk flask equipped with a magnetic stirrer the corresponding quantity (from 0.006 (1 mol %) to 0.6 mmol (100 mol %)) of  $(S_{M,R_C})-[(\eta^5\text{-C}_5\text{Me}_5)\text{M}\{(R)\text{-Prophos}\}(\text{H}_2\text{O})][\text{SbF}_6]_2$  (M = Rh (1), Ir (2)), solvent (4 mL), 0.90 mmol of *trans*- $\beta$ -nitrostyrene and about 100 mg of 4Å MS were added. The resulting mixture was stirred for 15 minutes at the selected temperature and then the corresponding indole (0.60 mmol) was added. After the appropriate reaction time, the reaction was quenched by addition of a methanolic solution of  $[\text{N}(n\text{Bu})_4]\text{Br}$ . The resulting suspension was vacuum-concentrated until dryness. The residue was extracted with  $\text{Et}_2\text{O}$  (4  $\times$  6 mL) and the resulting oil was analyzed by NMR and HPLC.

### Determination of the absolute configuration of 3u

At 263 K, a solution of *N*-methyl-2-methyl-3-(1-phenyl-2-nitroethyl)-indole (3u) (380.0 mg, 1.16 mmol, ee = 90 %) in THF (2 mL) and MeOH (7 mL) was mixed with a solution of KOH (76.6 mg, 1.16 mmol) in MeOH (15 mL). The mixture was stirred, at 263 K, for 20 min and a freshly prepared solution of  $\text{KMnO}_4$  (147.0 mg, 0.93 mmol) and  $\text{MgSO}_4$  (111.9 mg, 0.93 mmol) in  $\text{H}_2\text{O}$  (24 mL) were added dropwise, over 40 min. After one hour of additional stirring, the mixture was diluted with EtOAc (60 mL) and filtered through a pad of Celite. The Celite pad was washed with toluene (3  $\times$  30 mL). The combined filtrates were washed with brine (2  $\times$  30 mL) and  $\text{H}_2\text{O}$  (1  $\times$  30 mL), dried ( $\text{MgSO}_4$ ), filtered and the resulting solution was evaporated in vacuum to dryness. The obtained residue was immediately dissolved in 2-propanol (50 mL) and brought to 263 K. Then,  $\text{NaBH}_4$  (60 mg, 1.58 mmol) was added to the solution. The reaction was stirred at 263 K for 60 min and then neutralized with a saturated aqueous solution of  $[\text{N}(n\text{Bu})_4]\text{Cl}$ . The insoluble materials were removed by filtration,  $\text{H}_2\text{O}$  (10 mL) was added to the filtrate and the organic compounds were extracted with EtOAc (3  $\times$  60 mL). The combined extracts were dried ( $\text{MgSO}_4$ ), filtered and the solution evaporated in vacuum until dryness. The residue was loaded on a silica gel column and eluted first with hexane/EtOAc (9/1) and then, with hexane/EtOAc (7/3). After evaporation of the selected fractions, 2-(1,2-dimethyl-indol-3-yl)2-phenylethan-1-ol was obtained as a colorless syrup (127.7 mg, 37 %). The absolute configuration of the alcohol derivative was established as S by comparison of their optical properties with those reported in the literature.<sup>[22]</sup>  $[\alpha]_D^{25} = 33.4$  (c 1.4,  $\text{CHCl}_3$ ); ee = 89 %, determined by HPLC with a Chiralpak OD-H column (85/15, *n*-hexane/*i*PrOH; 1 mL/min;  $t_S = 28.2$  min (major),  $t_R = 33.0$  min (minor)).  $^1\text{H}$  NMR (300.13 MHz,  $\text{CDCl}_3$ , RT):  $\delta = 7.50$  (d,  $J = 8.0$  Hz, 1H,  $\text{H}_{Ar}$ ), 7.39 - 7.14 (m, 7H,  $\text{H}_{Ar}$ ), 7.04 (dt,  $J = 1.1$  and 7.1 Hz, 1H,  $\text{H}_{Ar}$ ), 4.54 (pt,  $J = 7.7$

Hz, 1H,  $\text{H}_\beta$ ), 5.23 (m, 2H, 2  $\times$   $\text{H}_\alpha$ ), 3.71 (s, 3H, NMe), 2.41 (s, 3H, Me), 1.57 ppm (brs, 1H, OH).  $^{13}\text{C}\{^1\text{H}\}$  NMR (75.48 MHz,  $\text{CDCl}_3$ , RT):  $\delta = 141.93$  ( $\text{C}_{Ar}$ ), 136.99 ( $\text{C}_{Ar}$ ), 135.21 ( $\text{C}_{Ar}$ ), 128.41 (2  $\times$   $\text{CH}_{Ar}$ ), 127.92 (2  $\times$   $\text{CH}_{Ar}$ ), 126.73 ( $\text{C}_{Ar}$ ), 126.26 ( $\text{CH}_{Ar}$ ), 120.73 ( $\text{CH}_{Ar}$ ), 119.28 ( $\text{CH}_{Ar}$ ), 119.19 ( $\text{CH}_{Ar}$ ), 109.32 ( $\text{C}_{Ar}$ ), 108.89 ( $\text{CH}_{Ar}$ ), 65.19 ( $\text{C}_\alpha$ ), 45.45 ( $\text{C}_\beta$ ), 29.65 (NMe), 10.70 ppm (Me).

### General procedure for the preparation of 4a-d and 5a,d

In an NMR tube, at 193 K to a suspension of  $(S_{M,R_C})-[(\eta^5\text{-C}_5\text{Me}_5)\text{M}\{(R)\text{-Prophos}\}(\text{H}_2\text{O})][\text{SbF}_6]_2$  (M = Rh (1), Ir (2)) (0.024 mmol) in  $\text{CD}_2\text{Cl}_2$  (0.45 mL), the corresponding *trans*- $\beta$ -nitrostyrene (0.024 mmol) and 4 Å MS (15 mg) were added. The resulting solution containing complexes 4a-d and 5a,d was analyzed by NMR without any further purification. Crystals suitable for X-ray analysis of 4d were obtained by crystallization from  $\text{CD}_2\text{Cl}_2$ /pentane solutions.

**$(S_{Rh,R_C})-[(\eta^5\text{-C}_5\text{Me}_5)\text{Rh}\{(R)\text{-Prophos}\}(\text{trans-}\beta\text{-nitrostyrene})][\text{SbF}_6]_2$  (4a).**  $^1\text{H}$  NMR (300.13 MHz,  $\text{CD}_2\text{Cl}_2$ , 213 K):  $\delta = 7.80$  - 7.18 (m, 25H,  $\text{H}_{Ar}$ ), 7.18 (brd,  $J(\text{H,H}) = 13.4$  Hz, 1H,  $\text{H}_\alpha$ ), 6.99 (brd,  $J(\text{H,H}) = 13.4$  Hz, 1H,  $\text{H}_\beta$ ), 3.55 (dt,  $J(\text{P,H}) = 53.4$  Hz and 13.8 Hz, 1H,  $\text{H}_{21}$ ), 3.12 (m, 1H,  $\text{H}_{11}$ ), 2.63 (t,  $J(\text{H,H}) = 14.6$  Hz, 1H,  $\text{H}_{22}$ ), 1.39 (pt,  $J(\text{H,H}) = 3.3$  Hz, 15H,  $\text{C}_5\text{Me}_5$ ), 1.24 ppm (dd,  $J(\text{P,H}) = 13.6$  and 6.0 Hz, 3H, Me).  $^{13}\text{C}\{^1\text{H}\}$  NMR (75.48 MHz,  $\text{CD}_2\text{Cl}_2$ , 213 K):  $\delta = 135.63$  - 120.82 (Ar), 146.97 (s,  $\text{C}_\beta$ ), 134.21 (s,  $\text{C}_\alpha$ ), 107.20 (brs,  $\text{C}_5\text{Me}_5$ ), 33.13 (dd,  $J(\text{P,C}) = 29.0$  and 8.7 Hz,  $\text{C}_2$ ), 31.07 (dd,  $J(\text{P,C}) = 32.1$  and 9.9 Hz,  $\text{C}_1$ ), 15.81 (dd,  $J(\text{P,C}) = 18.2$  and 5.2 Hz, Me), 10.12 ppm (s,  $\text{C}_5\text{Me}_5$ ).  $^{31}\text{P}\{^1\text{H}\}$  NMR (121.42 MHz,  $\text{CD}_2\text{Cl}_2$ , 213 K):  $\delta = 75.82$  (dd,  $J(\text{Rh,P}) = 130.6$  Hz,  $J(\text{P,P}) = 38.3$  Hz,  $\text{P}_1$ ), 51.52 ppm (dd,  $J(\text{Rh,P}) = 132.9$  Hz,  $\text{P}_2$ ).

**$(S_{Rh,R_C})-[(\eta^5\text{-C}_5\text{Me}_5)\text{Rh}\{(R)\text{-Prophos}\}(\text{trans-3-methoxy-}\beta\text{-nitrostyrene})][\text{SbF}_6]_2$  (4b).**  $^1\text{H}$  NMR (300.13 MHz,  $\text{CD}_2\text{Cl}_2$ , 213 K):  $\delta = 7.79$  - 6.84 (m, 24H,  $\text{H}_{Ar}$ ), 7.19 (d,  $J(\text{H,H}) = 13.4$  Hz, 1H,  $\text{H}_\alpha$ ), 6.89 (brd,  $J(\text{H,H}) = 13.3$  Hz, 1H,  $\text{H}_\beta$ ), 3.80 (s, 3H, OMe), 3.57 (dm,  $J(\text{P,H}) = 52.6$  Hz, 1H,  $\text{H}_{21}$ ), 3.14 (m, 1H,  $\text{H}_{11}$ ), 2.65 (m, 1H,  $\text{H}_{22}$ ), 1.37 (pt,  $J(\text{P,H}) = 3.1$  Hz, 15H,  $\text{C}_5\text{Me}_5$ ), 1.24 ppm (dd,  $J(\text{P,H}) = 14.0$  and 8.1 Hz, 3H, Me).  $^{13}\text{C}\{^1\text{H}\}$  NMR (75.48 MHz,  $\text{CD}_2\text{Cl}_2$ , 213 K):  $\delta = 159.91$  - 114.07 (Ar), 146.93 (s,  $\text{C}_\beta$ ), 134.27 (s,  $\text{C}_\alpha$ ), 107.35 (brs,  $\text{C}_5\text{Me}_5$ ), 55.80 (s, OMe), 33.34 (dd,  $J(\text{P,C}) = 32.5$  and 14.2 Hz,  $\text{C}_2$ ), 31.19 (dd,  $J(\text{P,C}) = 31.4$  and 10.5 Hz,  $\text{C}_1$ ), 15.97 (dd,  $J(\text{P,C}) = 18.1$  and 5.2 Hz, Me), 10.02 ppm (s,  $\text{C}_5\text{Me}_5$ ).  $^{31}\text{P}\{^1\text{H}\}$  NMR (121.42 MHz,  $\text{CD}_2\text{Cl}_2$ , 213 K):  $\delta = 75.76$  (dd,  $J(\text{Rh,P}) = 130.6$  Hz,  $J(\text{P,P}) = 38.3$  Hz,  $\text{P}_1$ ), 51.59 ppm (dd,  $J(\text{Rh,P}) = 133.1$  Hz,  $\text{P}_2$ ).

**$(S_{Rh,R_C})-[(\eta^5\text{-C}_5\text{Me}_5)\text{Rh}\{(R)\text{-Prophos}\}(\text{trans-4-methyl-}\beta\text{-nitrostyrene})][\text{SbF}_6]_2$  (4c).**  $^1\text{H}$  NMR (300.13 MHz,  $\text{CD}_2\text{Cl}_2$ , 213 K):  $\delta = 7.79$  - 6.83 (m, 24H,  $\text{H}_{Ar}$ ), 7.17 (d,  $J(\text{H,H}) = 13.3$  Hz, 1H,  $\text{H}_\alpha$ ), 6.95 (brd,  $J(\text{H,H}) = 13.3$  Hz, 1H,  $\text{H}_\beta$ ), 3.35 (dm,  $J(\text{P,H}) = 53.4$  Hz, 1H,  $\text{H}_{21}$ ), 3.11 (m, 1H,  $\text{H}_{11}$ ), 2.63 (m, 1H,  $\text{H}_{22}$ ), 2.37 (s, 3H, Me), 1.39 (pt,  $J(\text{P,H}) = 3.1$  Hz, 15H,  $\text{C}_5\text{Me}_5$ ), 1.22 ppm (m, 3H, Me).  $^{13}\text{C}\{^1\text{H}\}$  NMR (75.48 MHz,  $\text{CD}_2\text{Cl}_2$ , 213 K):  $\delta = 148.28$  - 120.97 (Ar), 147.41 (s,  $\text{C}_\beta$ ), 134.2 (s,  $\text{C}_\alpha$ ), 107.17 (brs,  $\text{C}_5\text{Me}_5$ ), 33.29 (dd,  $J(\text{P,C}) = 34.9$  and 13.0 Hz,  $\text{C}_2$ ), 31.21 (dd,  $J(\text{P,C}) = 31.3$  and 10.1 Hz,  $\text{C}_1$ ), 22.41 (s, Me), 15.88 (dd,  $J(\text{P,C}) = 17.9$  and 3.8 Hz, Me), 10.18 ppm (s,  $\text{C}_5\text{Me}_5$ ).  $^{31}\text{P}\{^1\text{H}\}$  NMR (121.42 MHz,  $\text{CD}_2\text{Cl}_2$ , 213 K):  $\delta = 75.81$  (dd,  $J(\text{Rh,P}) = 130.4$  Hz,  $J(\text{P,P}) = 38.4$  Hz,  $\text{P}_1$ ), 51.44 ppm (dd,  $J(\text{Rh,P}) = 132.7$  Hz,  $\text{P}_2$ ).

**$(S_{Rh,R_C})-[(\eta^5\text{-C}_5\text{Me}_5)\text{Rh}\{(R)\text{-Prophos}\}(\text{trans-4-chloro-}\beta\text{-nitrostyrene})][\text{SbF}_6]_2$  (4d).**  $^1\text{H}$  NMR (300.13 MHz,  $\text{CD}_2\text{Cl}_2$ , 213 K):  $\delta = 7.79$  - 7.21 (m, 24H,  $\text{H}_{Ar}$ ), 7.16 (d,  $J(\text{H,H}) = 13.4$  Hz, 1H,  $\text{H}_\alpha$ ), 6.94 (brd,  $J(\text{H,H}) = 13.4$  Hz, 1H,  $\text{H}_\beta$ ), 3.56 (dt,  $J(\text{P,H}) = 51.8$  Hz,  $J(\text{H,H}) = 11.8$  Hz, 1H,  $\text{H}_{21}$ ), 3.16 (m, 1H,  $\text{H}_{11}$ ), 2.65 (t,  $J(\text{H,H}) = 13.6$  Hz, 1H,  $\text{H}_{22}$ ), 1.38 (brs, 15H,  $\text{C}_5\text{Me}_5$ ), 1.24 ppm (dd,  $J(\text{P,H}) = 14.2$  and 7.1 Hz, 3H, Me).  $^{13}\text{C}\{^1\text{H}\}$  NMR (75.48 MHz,  $\text{CD}_2\text{Cl}_2$ , 213 K):  $\delta = 141.58$  - 120.97 (Ar), 145.46 (s,  $\text{C}_\beta$ ), 134.57 (s,  $\text{C}_\alpha$ ), 107.22 (brs,  $\text{C}_5\text{Me}_5$ ), 32.20 (m,  $\text{C}_2$ ), 31.14 (m,  $\text{C}_1$ ), 15.88 (dd,  $J(\text{P,C}) = 17.8$  and 5.3 Hz, Me), 10.20 ppm (s,  $\text{C}_5\text{Me}_5$ ).  $^{31}\text{P}\{^1\text{H}\}$  NMR (121.42 MHz,  $\text{CD}_2\text{Cl}_2$ ,

213 K):  $\delta = 75.89$  (dd,  $J(\text{Rh},\text{P}) = 130.6$  Hz,  $J(\text{P},\text{P}) = 38.1$  Hz,  $\text{P}_1$ ), 51.66 ppm (dd,  $J(\text{Rh},\text{P}) = 132.9$  Hz,  $\text{P}_2$ ).

**( $S_{\text{Rh}}$ ,  $R_{\text{C}}$ )-[( $\eta^5$ - $\text{C}_5\text{Me}_5$ ) $\text{Ir}\{(\text{R})\text{-Prophos}\}(\text{trans-}\beta\text{-nitrostyrene})]$  [ $\text{SbF}_6$ ]<sub>2</sub> (**5a**).  $^1\text{H}$  NMR (300.13 MHz,  $\text{CD}_2\text{Cl}_2$ , 213 K):  $\delta = 7.90$  - 7.30 (m, 25H,  $\text{H}_{\text{Ar}}$ ), 7.26 (brd,  $J(\text{H},\text{H}) = 13.2$  Hz, 1H,  $\text{H}_\alpha$ ), 7.15 (brd, 1H,  $\text{H}_\beta$ ), 3.51 (dt,  $J(\text{P},\text{H}) = 48.2$  Hz and 10.8 Hz, 1H,  $\text{H}_{21}$ ), 3.05 (m, 1H,  $\text{H}_{11}$ ), 2.55 (t,  $J(\text{H},\text{H}) = 17.2$  Hz, 1H,  $\text{H}_{22}$ ), 1.45 (br, 15H,  $\text{C}_5\text{Me}_5$ ), 1.26 ppm (dd,  $J(\text{P},\text{H}) = 14.4$  and 5.9 Hz, 3H, Me).  $^{13}\text{C}\{^1\text{H}\}$  NMR (75.48 MHz,  $\text{CD}_2\text{Cl}_2$ , 213 K):  $\delta = 136.18$  - 122.24 (Ar), 148.23 (s,  $\text{C}_\beta$ ), 134.40 (s,  $\text{C}_\alpha$ ), 101.18 (brs,  $\text{C}_5\text{Me}_5$ ), 33.13 (br,  $\text{C}_2$ ), 31.50 (dd,  $J(\text{P},\text{C}) = 37.1$  and 6.9 Hz,  $\text{C}_1$ ), 14.79 (dd,  $J(\text{P},\text{C}) = 18.6$  and 3.0 Hz, Me), 9.79 ppm (s,  $\text{C}_5\text{Me}_5$ ).  $^{31}\text{P}\{^1\text{H}\}$  NMR (121.42 MHz,  $\text{CD}_2\text{Cl}_2$ , 213 K):  $\delta = 49.02$  (d,  $J(\text{P},\text{P}) = 10.0$  Hz,  $\text{P}^1$ ), 28.00 ppm (d,  $\text{P}^2$ ).**

**( $S_{\text{Rh}}$ ,  $R_{\text{C}}$ )-[( $\eta^5$ - $\text{C}_5\text{Me}_5$ ) $\text{Ir}\{(\text{R})\text{-Prophos}\}(\text{trans-4-chloro-}\beta\text{-nitrostyrene})]$  [ $\text{SbF}_6$ ]<sub>2</sub> (**5d**).  $^1\text{H}$  NMR (300.13 MHz,  $\text{CD}_2\text{Cl}_2$ , 213 K):  $\delta = 8.03$  - 7.45 (m, 24H,  $\text{H}_{\text{Ar}}$ ), 7.23 (brd, 1H,  $\text{H}_\alpha$ ), 7.16 (brd, 1H,  $\text{H}_\beta$ ), 3.55 (dt,  $J(\text{P},\text{H}) = 48.7$  Hz and 11.8 Hz, 1H,  $\text{H}_{21}$ ), 3.09 (m, 1H,  $\text{H}_{11}$ ), 2.56 (t,  $J(\text{H},\text{H}) = 17.7$  Hz, 1H,  $\text{H}_{22}$ ), 1.49 (brt, 15H,  $\text{C}_5\text{Me}_5$ ), 1.25 ppm (dd,  $J(\text{P},\text{H}) = 14.3$  and 5.9 Hz, 3H, Me).  $^{13}\text{C}\{^1\text{H}\}$  NMR (75.48 MHz,  $\text{CD}_2\text{Cl}_2$ , 213 K):  $\delta = 146.65$  (s,  $\text{C}_\beta$ ), 136.18 - 122.24 (Ar), 132.34 (s,  $\text{C}_\alpha$ ), 101.17 (brs,  $\text{C}_5\text{Me}_5$ ), 33.13 (brdd,  $\text{C}_2$ ), 31.44 (dd,  $J(\text{P},\text{C}) = 36.9$  and 8.4 Hz,  $\text{C}_1$ ), 14.77 (dd,  $J(\text{P},\text{C}) = 17.2$  and 5.0 Hz, Me), 9.82 ppm (s,  $\text{C}_5\text{Me}_5$ ).  $^{31}\text{P}\{^1\text{H}\}$  NMR (121.42 MHz,  $\text{CD}_2\text{Cl}_2$ , 213 K):  $\delta = 48.66$  (d,  $J(\text{P},\text{P}) = 9.9$  Hz,  $\text{P}^1$ ), 27.88 ppm (d,  $\text{P}^2$ ).**

#### Procedure for the synthesis of **6**

In an NMR tube, at 193 K, to a suspension of ( $S_{\text{Rh}}$ ,  $R_{\text{C}}$ )-[( $\eta^5$ - $\text{C}_5\text{Me}_5$ ) $\text{Rh}\{(\text{R})\text{-Prophos}\}(\text{H}_2\text{O})$ ][ $\text{SbF}_6$ ]<sub>2</sub> (**1**) (20.0 mg, 0.016 mmol) in  $\text{CD}_2\text{Cl}_2$  (0.3 mL), *trans*- $\beta$ -nitrostyrene (2.4 mg, 0.016 mmol) and 4 Å MS (15 mg) were added. After 20 min, to the resulting solution *N*-methyl-2-methylindole (7.0 mg, 0.048 mmol) in  $\text{CD}_2\text{Cl}_2$  (0.15 mL) was added, at 193 K. The resulting solution was analyzed by NMR without any further purification and showed the presence of complexes **6** in 70/30, **6a/6b** molar ratio. HRMS (ESI):  $m/z$ : 943.2987 (Calc. 943.3023 [ $\text{C}_{55}\text{H}_{58}\text{N}_2\text{O}_2\text{P}_2\text{Rh}$ ]<sup>+</sup>).

**6a.**  $^1\text{H}$  NMR (300.13 MHz,  $\text{CD}_2\text{Cl}_2$ , 193 K):  $\delta = 17.5$  (br, 1H, OH), 6.22 (d,  $J = 7.6$  Hz, 1H,  $\text{H}_\alpha$ ), 5.29 (d,  $J = 7.6$  Hz, 1H,  $\text{H}_\beta$ ), 3.73 (brs, 3H, NMe), 2.64 (s, 3H, Me), 1.26 (brs, 15H,  $\text{C}_5\text{Me}_5$ ), 0.92 ppm (br, 3H, Me).  $^{13}\text{C}\{^1\text{H}\}$  NMR (75.48 MHz,  $\text{CD}_2\text{Cl}_2$ , 193 K):  $\delta = 118.43$  ( $\text{C}_\alpha$ ), 38.79 ( $\text{C}_\beta$ ), 34.60 (NMe), 17.29 (Me<sub>indole</sub>), 14.53 (br, Me), 9.07 ppm (s,  $\text{C}_5\text{Me}_5$ ).  $^{31}\text{P}\{^1\text{H}\}$  NMR (121.42 MHz,  $\text{CD}_2\text{Cl}_2$ , 193 K):  $\delta = 75.90$  (dd,  $J(\text{Rh},\text{P}) = 130.5$  Hz,  $J(\text{P},\text{P}) = 43.2$  Hz,  $\text{P}_1$ ), 50.23 ppm (dd,  $J(\text{Rh},\text{P}) = 132.2$  Hz,  $\text{P}_2$ ).

**6b.**  $^1\text{H}$  NMR (300.13 MHz,  $\text{CD}_2\text{Cl}_2$ , 193 K):  $\delta = 17.5$  (br, 1H, OH), 6.10 (brd,  $J = 6.4$  Hz, 1H,  $\text{H}_\alpha$ ), 4.81 (brd,  $J = 6.4$  Hz, 1H,  $\text{H}_\beta$ ), 3.73 (brs, 3H, NMe), 2.46 (s, 3H, Me), 1.30 (brs, 15H,  $\text{C}_5\text{Me}_5$ ), 1.11 ppm (br, 3H, Me).  $^{13}\text{C}\{^1\text{H}\}$  NMR (75.48 MHz,  $\text{CD}_2\text{Cl}_2$ , 193 K):  $\delta = 113.70$  ( $\text{C}_\alpha$ ), 40.62 ( $\text{C}_\beta$ ), 30.30 (NMe), 11.08 (Me<sub>indole</sub>), 14.80 (br, Me), 9.17 ppm (s,  $\text{C}_5\text{Me}_5$ ).  $^{31}\text{P}\{^1\text{H}\}$  NMR (121.42 MHz,  $\text{CD}_2\text{Cl}_2$ , 193 K):  $\delta = 76.84$  (brdd,  $J(\text{Rh},\text{P}) = 132.8$  Hz,  $J(\text{P},\text{P}) = 42.5$  Hz,  $\text{P}_1$ ), 51.80 ppm (brdd,  $J(\text{Rh},\text{P}) = 134.8$  Hz,  $\text{P}_2$ ).

#### Preparation of the *aci*-nitro compounds **7** and **7d**

At 193 K, in an NMR tube, to a suspension of ( $S_{\text{Rh}}$ ,  $R_{\text{C}}$ )-[( $\eta^5$ - $\text{C}_5\text{Me}_5$ ) $\text{Rh}\{(\text{R})\text{-Prophos}\}(\text{H}_2\text{O})$ ][ $\text{SbF}_6$ ]<sub>2</sub> (**1**) (12.4 mg, 0.010 mmol) in  $\text{CD}_2\text{Cl}_2$  (0.3 mL), the corresponding nitrostyrene (0.30 mmol) and 4 Å MS (15 mg) were added. After 20 min, to the resulting solution *N*-methyl-2-methylindole (0.20 mmol) in  $\text{CD}_2\text{Cl}_2$  (0.15 mL) was added. The gradual consumption of the indole with the concomitant appearance of the *aci*-nitro compound was monitored by NMR at 233 K. When the indole was not observed, the compounds **7** (*trans*- $\beta$ -nitrostyrene) and **7d**

(*trans*-4-chloro- $\beta$ -nitrostyrene) were fully characterized by NMR at 223 K in the presence of **3u** and **3ag**, respectively (7/3u molar ratio: 85/15; 7d/3ag molar ratio: 70/30). Small amounts of complexes **6** were also present but not observable by  $^1\text{H}$  NMR at 223 K.

**7.**  $^1\text{H}$  NMR (300.13 MHz,  $\text{CD}_2\text{Cl}_2$ , 223 K):  $\delta = 13.6$  (br, 1H, OH), 7.65 - 6.86 (m, 9H,  $\text{H}_{\text{Ar}}$ ), 7.03 (d,  $J = 8.1$  Hz, 1H,  $\text{H}_\alpha$ ), 5.58 (d,  $J = 8.1$  Hz, 1H,  $\text{H}_\beta$ ), 3.66 (s, 3H, NMe), 2.44 ppm (s, 3H, Me).  $^{13}\text{C}\{^1\text{H}\}$  NMR (75.48 MHz,  $\text{CD}_2\text{Cl}_2$ , 223 K):  $\delta = 139.96$  ( $\text{C}_{\text{Ph}}$ ), 137.06 ( $\text{C}_9$ ), 135.71 ( $\text{C}_2$ ), 128.97 (2  $\times$   $\text{CH}_{\text{Ph}}$ ), 127.63 (2  $\times$   $\text{CH}_{\text{Ph}}$ ), 127.24 ( $\text{CH}_{\text{Ph}}$ ), 125.99 ( $\text{C}_8$ ), 122.43 ( $\text{C}_\alpha$ ), 121.09 ( $\text{C}_4$ ), 119.33 ( $\text{C}_5$ ), 118.74 ( $\text{C}_6$ ), 109.48 ( $\text{C}_7$ ), 107.67 ( $\text{C}_3$ ), 39.31 ( $\text{C}_\beta$ ), 30.19 (NMe), 10.99 ppm (Me).

**7d.**  $^1\text{H}$  NMR (500.13 MHz,  $\text{CD}_2\text{Cl}_2$ , 223 K):  $\delta = 13.5$  (br, 1H, OH), 7.53 - 6.91 (m, 8H,  $\text{H}_{\text{Ar}}$ ), 6.97 (d,  $J = 8.0$  Hz, 1H,  $\text{H}_\alpha$ ), 5.53 (d,  $J = 8.0$  Hz, 1H,  $\text{H}_\beta$ ), 3.67 (s, 3H, NMe), 2.43 ppm (s, 3H, Me).  $^{13}\text{C}\{^1\text{H}\}$  NMR (125.77 MHz,  $\text{CD}_2\text{Cl}_2$ , 223 K):  $\delta = 138.51$  ( $\text{C}_{\text{Ph}}$ ), 137.05 ( $\text{C}_9$ ), 135.95 ( $\text{C}_2$ ), 132.62 ( $\text{C}_{\text{Cl}}$ ), 129.13 (2  $\times$   $\text{CH}_{\text{Ph}}$ ), 128.92 (2  $\times$   $\text{CH}_{\text{Ph}}$ ), 125.74 ( $\text{C}_8$ ), 121.87 ( $\text{C}_\alpha$ ), 121.16 ( $\text{C}_4$ ), 119.39 ( $\text{C}_5$ ), 118.61 ( $\text{C}_6$ ), 109.52 ( $\text{C}_7$ ), 107.15 ( $\text{C}_3$ ), 38.74 ( $\text{C}_\beta$ ), 30.24 (NMe), 11.01 ppm (Me).

#### Procedure for the preparation of [( $\eta^5$ - $\text{C}_5\text{Me}_5$ ) $\text{Rh}\{(\text{R})\text{-Prophos}\}(\text{3u})]$ [ $\text{SbF}_6$ ]<sub>2</sub> (**8**)

At 193 K, in an NMR tube, to a suspension of ( $S_{\text{Rh}}$ ,  $R_{\text{C}}$ )-[( $\eta^5$ - $\text{C}_5\text{Me}_5$ ) $\text{Rh}\{(\text{R})\text{-Prophos}\}(\text{H}_2\text{O})$ ][ $\text{SbF}_6$ ]<sub>2</sub> (**1**) (20.0 mg, 0.016 mmol) in  $\text{CD}_2\text{Cl}_2$  (0.4 mL), racemic **3u** (47.2 mg, 0.16 mmol) and 4 Å MS (15 mg) were added. The resulting solution was analyzed by NMR without any further purification and consist of a mixture of complexes **8** and **1**, in 75/25, **8/1** and 65/35, **8a/8b** molar ratio.

**8a.**  $^1\text{H}$  NMR (300.13 MHz,  $\text{CD}_2\text{Cl}_2$ , 193 K):  $\delta = 4.88$  (m), 4.61 - 4.35 ppm (m, 3H, 2  $\times$   $\text{H}_\alpha$ , 1 $\text{H}_\beta$ ).  $^{31}\text{P}\{^1\text{H}\}$  NMR (121.42 MHz,  $\text{CD}_2\text{Cl}_2$ , 193 K):  $\delta = 72.88$  (dd,  $J(\text{Rh},\text{P}) = 131.2$  Hz,  $J(\text{P},\text{P}) = 38.6$  Hz,  $\text{P}^1$ ), 48.80 ppm (dd,  $J(\text{Rh},\text{P}) = 132.2$  Hz,  $\text{P}^2$ ).

**8b.**  $^1\text{H}$  NMR (300.13 MHz,  $\text{CD}_2\text{Cl}_2$ , 193 K):  $\delta = 4.61$  - 4.35 (m), 4.03 ppm (m, 3H, 2  $\times$   $\text{H}_\alpha$ , 1 $\text{H}_\beta$ ).  $^{31}\text{P}\{^1\text{H}\}$  NMR (121.42 MHz,  $\text{CD}_2\text{Cl}_2$ , 193 K):  $\delta = 74.58$  (brdd,  $J(\text{Rh},\text{P}) = 132.7$  Hz,  $J(\text{P},\text{P}) = 37.4$  Hz,  $\text{P}^1$ ), 50.38 ppm (brdd,  $J(\text{Rh},\text{P}) = 132.6$  Hz,  $\text{P}^2$ ).

#### NMR study of the reversibility of the cycle **A**

**a)** At 193 K, in an NMR tube, to a suspension of the complex ( $S_{\text{Rh}}$ ,  $R_{\text{C}}$ )-[( $\eta^5$ - $\text{C}_5\text{Me}_5$ ) $\text{Rh}\{(\text{R})\text{-Prophos}\}(\text{H}_2\text{O})$ ][ $\text{SbF}_6$ ]<sub>2</sub> (**1**) (7.0 mg, 0.006 mmol) in  $\text{CD}_2\text{Cl}_2$  (0.3 mL), *trans*- $\beta$ -nitrostyrene (22.3 mg, 0.150 mmol) and 4 Å MS (15 mg) were added. After 20 min, to the resulting solution *N*-methyl-2-methylindole (17.5 mg, 0.120 mmol) in  $\text{CD}_2\text{Cl}_2$  (0.15 mL) was added, at the same temperature. Then, the gradual consumption of the indole with the concomitant appearance of the *aci*-nitro compound **7** was monitored by NMR at 233 K. The *N*-methyl-2-methylindole was progressively reacting and when it was not detectable by  $^1\text{H}$  NMR, the solution consisted of a 7/3u mixture in an 85/15 molar ratio. Then, at the same temperature, 27.5 mg (0.150 mmol) of *trans*-4-chloro- $\beta$ -nitrostyrene were added and the  $^1\text{H}$  NMR showed the instantaneous formation of **7d** in a 7/7d molar ratio of 40/60. Heating up to 298 K, **7** and **7d** evolved to the corresponding FC products **3u** and **3ag**, respectively, which are formed in a 60/40 molar ratio.

**b)** In an NMR tube, at 193K, to a suspension of ( $S_{\text{Rh}}$ ,  $R_{\text{C}}$ )-[( $\eta^5$ - $\text{C}_5\text{Me}_5$ ) $\text{Rh}\{(\text{R})\text{-Prophos}\}(\text{H}_2\text{O})$ ][ $\text{SbF}_6$ ]<sub>2</sub> (**1**) (7.0 mg, 0.006 mmol) in  $\text{CD}_2\text{Cl}_2$  (0.3 mL), *trans*- $\beta$ -nitrostyrene (26.9 mg, 0.180 mmol) and 4 Å MS (15 mg) were added. After 20 min, to the resulting solution



*N*-methyl-2-methylindole (17.5 mg, 0.120 mmol) in CD<sub>2</sub>Cl<sub>2</sub> (0.15 mL) was added, at the same temperature. In two independent experiments, the solution was monitored by NMR at 253 K and at 273 K. The spectra show constants  $\tau$ /indole molar ratios of 94/6 and 70/30 at 253 K and 273 K, respectively.

#### Kinetic studies for the step 6 → 8

In an NMR tube, at 193 K, to solid (S<sub>Rh</sub>,R<sub>C</sub>)-[( $\eta^5$ -C<sub>5</sub>Me<sub>5</sub>)Rh{(R)-Prophos}(H<sub>2</sub>O)](SbF<sub>6</sub>)<sub>2</sub> (**1**) (4.01 mg, 5.95 mg, 7.02 mg and 9.72 mg, respectively) and 4 Å MS (15 mg), a solution of *trans*- $\beta$ -nitrostyrene in CD<sub>2</sub>Cl<sub>2</sub> (0.3 mL, 241.96 mM) was added. After 20 min, to the resulting solution *N*-methyl-2-methylindole in CD<sub>2</sub>Cl<sub>2</sub> (0.3 mL, 161.39 mM) was added, at the same temperature. Then, the gradual consumption of the indole with the concomitant appearance of the *aci*-nitro compound **7** was monitored by NMR at 233 K. When the *N*-methyl-2-methylindole was not observed ( $t = 0$ ), kinetic data were acquired at 233 K. The concentrations of *aci*-nitro compound **7** and Friedel-Crafts product **3u** were assayed using the formula  $[\text{indole}]_0 = [\mathbf{7}] + [\mathbf{3u}] + [\mathbf{6}]$  where  $[\text{indole}]_0$  is the initial concentration of indole (80.69 mM) and  $[\mathbf{6}]$  is the concentration of *aci*-nitro complexes **6** corresponding to the catalyst loading (5.77 mM (7.2 mol %); 8.56 mM (10.6 mol %); 10.10 mM (12.5 mol %); 13.99 mM (17.3 mol %)). Kinetic parameters were obtained through Eyring analyses by measuring  $k_{\text{obs}}$  as a function of concentration of *aci*-nitro **7**.

#### Computational details

All DFT theoretical calculations have been carried out using the G09.D01 program package.<sup>[36]</sup> The B3LYP method<sup>[37]</sup> has been employed including the D3 dispersion correction proposed by Grimme<sup>[38]</sup> and the "ultrafine" grid. The def2-SVP basis set<sup>[39]</sup> has been selected for all atoms for geometry optimizations and calculation of free energy corrections at different temperatures. Dichloromethane solvent effects were introduced by the PCM continuum approach using single point energy calculations at the gas-phase optimized geometry.<sup>[40]</sup> Due to the excess of *trans*- $\beta$ -nitrostyrene in the reaction media and the well-known overestimation of translational entropy in solution as calculated by the gas phase approach, only the rotational and vibrational entropic terms have been considered for the *trans*- $\beta$ -nitrostyrene molecule. The nature of the stationary points has been confirmed by frequency calculations and the transition structures have been characterized by a single imaginary frequency corresponding to the expected motion of the atoms. The proton transfer in the 1,3- $\sigma$ -sigmatropic rearrangement of the *aci*-nitro compound is greatly favored by the presence of water molecules by means of a Grotthuss mechanism.<sup>[32]</sup> Two and three water molecules have been added for the conversion of **7** into **3u** and **6** into **8**, respectively, according to the probably presence of traces of water coming from the catalyst precursor.

#### Structural Analysis

X-ray diffraction data were collected at 100(2) K with graphite-monochromated Mo-K $\alpha$  radiation ( $\lambda = 0.71073$  Å), using narrow  $\omega$  rotation (0.3 °) on a Bruker SMART (**3w** compound) and a Bruker APEX DUO (**3x**, **3ah**, **4d** compounds) diffractometers. Intensities were integrated with SAINT+ program<sup>[41]</sup> and corrected for absorption effect with SADABS program<sup>[42]</sup> integrated in APEX2 package. The structures were solved by direct methods with SHELXS-2013<sup>[43]</sup> and refined, by full-matrix least-squares on  $F^2$ , with SHELXL-2014<sup>[44]</sup> included in WINGX package.<sup>[45]</sup> Hydrogen atoms were included in calculated positions and refined with displacement and positional riding parameters. CCDC 1459314, 1459329, 943405 and 943404 contain the supplementary crystallographic data for

complexes **3w**, **3x**, **3ah** and **4d**, respectively. These data can be obtained free of charge from the Cambridge Crystallographic Data Centre.

Due to the temperature-sensitivity of **4d**, the isolation and measurement of the sample required careful manipulation at low temperature (below 233 K) through the whole process. Single crystals were picked out from the mother solution in a small spoon well covered by Fomblin oil. They were quickly immersed in the inert oil on a microscope slide with a cavity surrounded by dry-ice blocks. The generated cool inert gas atmosphere maintained the crystal stability.

**Crystal data for 4d:** C<sub>45</sub>H<sub>47</sub>ClF<sub>12</sub>NO<sub>2</sub>P<sub>2</sub>RhSb<sub>2</sub>,  $M = 1305.64$ ; red prism, 0.070 × 0.075 × 0.148 mm<sup>3</sup>; monoclinic,  $P2_1$ ;  $a = 13.4677(12)$ ,  $b = 13.0152(12)$ ,  $c = 14.0491(13)$  Å;  $\beta = 101.833(2)^\circ$ ;  $Z = 2$ ;  $V = 2410.3(4)$  Å<sup>3</sup>;  $D_c = 1.799$  g/cm<sup>3</sup>;  $\mu = 1.658$  mm<sup>-1</sup>, minimum and maximum absorption correction factors 0.7178 and 0.8865;  $2\theta_{\text{max}} = 55.266^\circ$ ; 24892 collected reflections, 10174 unique ( $R_{\text{int}} = 0.0765$ ); number of data/restraints/parameters 10174/6/601; final GOF 0.969;  $R_1 = 0.0546$  (6180 reflections,  $I > 2\sigma(I)$ );  $wR2 = 0.1180$  for all data; Flack parameter 0.01(3). Restraints (DELU) concerning ADPs for 4 carbon atoms have been included in the refinement to avoid unrealistic values.

#### Acknowledgements

We thank the Ministerio de Educación y Competitividad (CTQ2012-32095 and CTQ2015-66079-P) and Gobierno de Aragón (Grupo Consolidado: Catalizadores Organometálicos Enantioselectivos) for financial support. This work was supported by the CONSOLIDER INGENIO-2010 program under the project "Factoría de Cristalización" (CSD2006-0015). I. M. acknowledges Ministerio de Economía y Competitividad of Spain for a FPI grant. I. M. and R. R. acknowledge CSIC, European Social Fund and Ministerio de Economía y Competitividad of Spain for a JAE and a Ramón y Cajal (RYC-2013-13800) grants. V. P. thanks the Ministerio de Economía y Competitividad of Spain (CTQ2012-35665 and CTQ2015-67366-P) and the resources from the supercomputer "Memento", and the technical expertise and assistance provided by the Institute for Biocomputation and Physics of Complex Systems (BIFI) Universidad de Zaragoza.

**Keywords:** catalytic mechanism • Friedel-Crafts reaction • indoles • nitroalkenes • rhodium

- [1] a) *Comprehensive Asymmetric Catalysis*, Vol 1-3 (Eds.: E. N. Jacobsen, A. Pfaltz, H. Yamamoto), Springer, New York, **1999**; Suppl. 1 and 2, Springer, New York, **2004**. b) *Catalytic Asymmetric Synthesis*, (Ed.: I. Ojima), VCH, Wiley-Weinheim, Germany, **2000**. c) R. Noyori in *Asymmetric Catalysis in Organic Synthesis*, John Wiley and Sons, New York, **1994**. d) P. J. Walsh, M. C. Kozlowski in *Fundamentals of Asymmetric Catalysis*, University Science Books, Sausalito, **2009**. [2] a) J. Escorihuela, M. I. Burguete, S. V. Luis, *Chem. Soc. Rev.* **2013**, *42*, 5595-5617. b) M. Bartók, *Chem. Rev.* **2010**, *110*, 1663-1705. c) T. Tanaka, M. Hayashi, *Synthesis* **2008**, 3361-3376. d) G. Zanoni, F. Castronovo, M. Francini, G. Vidari, E. Giannini, *Chem. Soc. Rev.* **2003**, *32*, 115-129. e) Y. H. Kim, *Acc. Chem. Res.* **2001**, *34*, 955-962. f) For a review discussing the isoinversion principle, see: H. Buschmann, H.-D. Scharf, N. Hoffmann, P. Esser, *Angew. Chem. Int. Ed. Engl.* **1991**, *30*, 477-515.



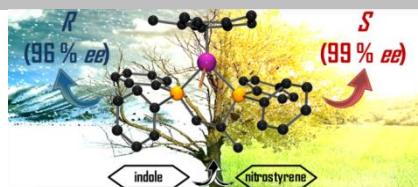
- [3] For metal-catalyzed processes, see for example: a) P. Pongrácz, T. Papp, L. Kollár, T. Kégl, *Organometallics* **2014**, *33*, 1389-1396 and references therein. b) V. S. Chan, M. Chiu, R. G. Bergman, F. D. Toste, *J. Am. Chem. Soc.* **2009**, *131*, 6021-6032. c) R. Saito, S. Naruse, K. Takano, K. Fukuda, A. Katoh, Y. Inoue, *Org. Lett.* **2006**, *8*, 2067-2070. d) C. P. Casey, S. C. Martins, M. A. Fagan, *J. Am. Chem. Soc.* **2004**, *126*, 5585-5592. e) M. P. Sibi, U. Gorikunti, M. Liu, *Tetrahedron* **2002**, *58*, 8357-8363. f) S. Kanemasa, Y. Oderaotoshi, E. Wada, *J. Am. Chem. Soc.* **1999**, *121*, 8675-8676. g) J. Otera, K. Sakamoto, T. Tsukamoto, A. Orita, *Tetrahedron Lett.* **1998**, *39*, 3201-3204. h) D. Sinou, *Tetrahedron Lett.* **1981**, *22*, 2987-2990.
- [4] In this context, a remarkable example in which epimerization of a rhodium catalyst, by changing the reaction temperature, provides access to both enantiomers of an asymmetric hydrogenation, has been recently reported: G. Storch, O. Trapp, *Angew. Chem. Int. Ed.* **2015**, *54*, 3580-3586.
- [5] M. Bandini, A. Umani-Ronchi in *Catalytic Asymmetric Friedel-Crafts Alkylations*, Wiley-VCH: Weinheim, Germany, **2009**.
- [6] R. Dalpozzo, *Chem. Soc. Rev.* **2015**, *44*, 742-778.
- [7] S. Lancianesi, A. Palmieri, M. Petrini, *Chem. Rev.* **2014**, *114*, 7108-7149.
- [8] M. Bandini, A. Garelli, M. Rovinetti, S. Tommasi, A. Umani-Ronchi, *Chirality* **2005**, *17*, 522-529.
- [9] a) T. Sato, T. Arai, *Synlett* **2014**, *25*, 349-354. b) T. Arai, Y. Yamamoto, A. Awata, K. Kamiya, M. Ishibashi, M. A. Arai, *Angew. Chem. Int. Ed.* **2013**, *52*, 2486-2490. c) T. Arai, A. Awata, M. Wasai, N. Yokoyama, H. Masu, *J. Org. Chem.* **2011**, *76*, 5450-5456. d) T. Arai, M. Wasai, N. Yokoyama, *J. Org. Chem.* **2011**, *76*, 2909-2912. e) J. Wu, X. Li, F. Wu, B. Wan, *Org. Lett.* **2011**, *13*, 4834-4837. f) H. Y. Kim, S. Kim, K. Oh, *Angew. Chem. Int. Ed.* **2010**, *49*, 4476-4478. g) N. Yokoyama, T. Arai, *Chem. Commun.* **2009**, 3285-3287. h) T. Arai, N. Yokoyama, *Angew. Chem. Int. Ed.* **2008**, *47*, 4989-4992; Corrigendum: *Angew. Chem. Int. Ed.* **2008**, *47*, 9555. i) Y. Sui, L. Liu, J.-L. Zhao, D. Wang, Y.-J. Chen, *Tetrahedron Lett.* **2007**, *63*, 5173-5183. j) P. K. Singh, A. Bisai, V. K. Singh, *Tetrahedron Lett.* **2007**, *48*, 1127-1129.
- [10] G. Zhang, *Inorg. Chem. Commun.* **2014**, *40*, 1-4.
- [11] a) G. V. More, B. M. Bhanage, *Catal. Sci. Technol.* **2015**, *5*, 1514-1520. b) W.-J. Li, *Catal. Commun.* **2014**, *52*, 53-56. c) M. S. Islam, A. M. A. Al Majid, Z. A. Al-Othman, A. Barakat, *Tetrahedron: Asymmetry* **2014**, *25*, 245-251. d) Y. Jia, W. Yang, D.-M. Du, *Org. Biomol. Chem.* **2012**, *10*, 4739-4746. e) J. Peng, D.-M. Du, *Eur. J. Org. Chem.* **2012**, 4042-4051. f) S. C. McKeon, H. Müller-Bunz, P. J. Guiry, *Eur. J. Org. Chem.* **2011**, 7107-7115. g) F. Guo, G. Lai, S. Xiong, S. Wang, Z. Wang, *Chem. Eur. J.* **2010**, *16*, 6438-6441. h) H. Liu, D.-M. Du, *Adv. Synth. Catal.* **2010**, *352*, 1113-1118. i) S. C. McKeon, H. Müller-Bunz, P. J. Guiry, *Eur. J. Org. Chem.* **2009**, 4833-4841. j) S.-z. Lin, T.-p. You, *Tetrahedron* **2009**, *65*, 1010-1016. k) Z.-L. Yuan, Z.-Y. Lei, M. Shi, *Tetrahedron: Asymmetry* **2008**, *19*, 1339-1346. l) H. Liu, S.-F. Lu, J. Xu, D.-M. Du, *Chem. Asian J.* **2008**, *3*, 1111-1121. m) S.-F. Lu, D.-M. Du, J. X. Xu, *Org. Lett.* **2006**, *8*, 2115-2118. n) Y.-X. Jia, S.-F. Zhu, Y. Yang, Q.-L. Zhou, *J. Org. Chem.* **2006**, *71*, 75-80.
- [12] a) H. Wu, R.-R. Liu, Y.-X. Jia, *Synlett* **2014**, *25*, 457-460. b) J.-Q. Weng, Q.-M. Deng, L. Wu, K. Xu, H. Wu, R.-R. Liu, J.-R. Gao, Y.-X. Jia, *Org. Lett.* **2014**, *16*, 776-779. c) J.-R. Gao, H. Wu, B. Xiang, W.-B. Yu, L. Han, Y.-X. Jia, *J. Am. Chem. Soc.* **2013**, *135*, 2983-2986.
- [13] a) X.-Q. Hao, Y.-X. Xu, M.-J. Yang, L. Wang, J.-L. Niu, J.-F. Gong, M.-P. Song, *Organometallics* **2012**, *31*, 835-846. b) L.-Y. Wu, X.-Q. Hao, Y.-X. Xu, M.-Q. Jia, Y.-N. Wang, J.-F. Gong, M.-P. Song, *Organometallics* **2009**, *28*, 3369-3380.
- [14] P. Drabina, B. Bröz, E. Padělková, M. Sedlák, *J. Organomet. Chem.* **2011**, *696*, 971-981.
- [15] a) D. Carmona, M. P. Lamata, F. Viguri, R. Rodríguez, L. A. Oro, A. I. Balana, F. J. Lahoz, T. Tejero, P. Merino, S. Franco, I. Montesa, *J. Am. Chem. Soc.* **2004**, *126*, 2716-2717. b) D. Carmona, M. P. Lamata, F. Viguri, R. Rodríguez, L. A. Oro, F. J. Lahoz, A. I. Balana, T. Tejero, P. Merino *J. Am. Chem. Soc.* **2005**, *127*, 13386-13398.
- [16] a) D. Carmona, F. Viguri, A. Asenjo, F. J. Lahoz, P. García-Orduña, L. A. Oro, *J. Mol. Catal. A Chemical* **2014**, *385*, 119-124. b) D. Carmona, F. Viguri, A. Asenjo, F. J. Lahoz, P. García-Orduña, L. A. Oro, *Organometallics* **2012**, *31*, 4551-4557. c) D. Carmona, F. Viguri, A. Asenjo, M. P. Lamata, F. J. Lahoz, P. García-Orduña, L. A. Oro, *Organometallics* **2011**, *30*, 6661-6673. d) D. Carmona, M. P. Lamata, F. Viguri, C. Barba, R. Rodríguez, F. J. Lahoz, M. L. Martín, L. A. Oro, L. Salvatella, *Organometallics* **2007**, *26*, 6493-6496. e) C. Barba, D. Carmona, J. I. García, M. P. Lamata, J. A. Mayoral, L. Salvatella, F. Viguri, *J. Org. Chem.* **2006**, *71*, 9831-9840. f) D. Carmona, C. Catiaviela, R. García-Correas, F. J. Lahoz, M. P. Lamata, J. A. López, M. P. López-Ram de Víu, L. A. Oro, E. San José, F. Viguri, *Chem. Commun.* **1996**, 1247-1248.
- [17] a) A. Asenjo, F. Viguri, M. P. Lamata, R. Rodríguez, M. Carmona, L. A. Oro, D. Carmona, *Catal. Sci. Technol.* **2015**, *5*, 2460, 2466. b) D. Carmona, M. P. Lamata, F. Viguri, R. Rodríguez, F. J. Lahoz, M. J. Fabra, L. A. Oro, *Tetrahedron: Asymmetry* **2009**, *20*, 1197-1205. c) D. Carmona, M. P. Lamata, F. Viguri, R. Rodríguez, F. J. Lahoz, L. A. Oro, *Chem. Eur. J.* **2007**, *13*, 9746-9756. d) D. Carmona, M. P. Lamata, F. Viguri, R. Rodríguez, T. Fischer, F. J. Lahoz, I. T. Dobrinovitch, L. A. Oro, *Adv. Synth. Catal.* **2007**, *349*, 1751-1758. e) D. Carmona, M. P. Lamata, F. Viguri, J. Ferrer, N. García, F. J. Lahoz, M. L. Martín, L. A. Oro, *Eur. J. Inorg. Chem.* **2006**, 3155-3166.
- [18] D. Carmona, M. P. Lamata, A. Sánchez, F. Viguri, L. A. Oro, *Tetrahedron: Asymmetry* **2011**, *22*, 893-906.
- [19] D. Carmona, I. Méndez, R. Rodríguez, F. J. Lahoz, P. García-Orduña, L. A. Oro, *Organometallics* **2014**, *33*, 443-446.
- [20] a) R. Ballini, M. Petrini, *Tetrahedron* **2004**, *60*, 1017-1047. b) K. Steliou, M.-A. Poupard, *J. Org. Chem.* **1985**, *50*, 4971-4973.
- [21] J. U. Nef, *Justus Liebigs Ann. Chem.* **1894**, *280*, 263-291.
- [22] M. Bandini, M. Fagioli, A. Melloni, A. Umani-Ronchi, *Adv. Synth. Catal.* **2004**, *346*, 573-578.
- [23] D. Carmona, F. J. Lahoz, L. A. Oro, M. P. Lamata, F. Viguri, E. San José, *Organometallics* **1996**, *15*, 2961-2966.
- [24] Y. Inoue, N. Yamasaki, T. Yokoyama, A. Tai, *J. Org. Chem.* **1992**, *57*, 1332-1345.
- [25] For plots of ee against reaction time at the temperatures quoted in Table 4, see SI.
- [26] An 1/30/20 catalyst precursor/nitroalkene/indole molar ratio was used in the catalytic experiments.
- [27] Priority sequence,  $\eta^5\text{-C}_5\text{Me}_5 > \text{P}(1) > \text{P}(2) > \text{O}$ : a) R. S. Cahn, C. Ingold, V. Prelog, *Angew. Chem., Int. Ed. Engl.* **1966**, *5*, 385-415; b) V. Prelog, G. Helmchen, *Angew. Chem., Int. Ed. Engl.* **1982**, *21*, 567-583. c) C. Lecomte, Y. Dusausoy, J. Protas, J. Tirouflet, A. Dormond, *J. Organomet. Chem.* **1974**, *73*, 67-76.
- [28] D. Cremer, J. A. Pople, *J. Am. Chem. Soc.* **1975**, *97*, 1354-1358.
- [29] M. Nishio, Y. Umezawa, J. Fantini, M. S. Weiss, P. Chakrabarti, *Phys. Chem. Chem. Phys.* **2014**, *16*, 12648-12683 and references therein.
- [30] For the complete NMR characterization of the *aci*-nitro complexes **6** and free *aci*-nitro **7**, see Experimental Section.
- [31] The spectra were recorded at 193 K because at 223 K the  $\text{H}_a$  and  $\text{H}_b$  protons of complexes **6** were not observed in the  $^1\text{H}$  NMR spectrum.
- [32] C. J. T. Grothuis, *Ann. Chim. (Paris)* **1806**, *58*, 54-73. Catalyst precursor **1** contains a coordinated water molecule and crystallizes with an additional water molecule (see ref. 15).
- [33] According to the theoretical calculations, the presence of a small amount of water facilitates the prototropic shifts. At this respect, we have observed that, at 233 K, the rate of reaction between *N*-methyl-2-methylindole and *trans*- $\beta$ -nitrostyrene, without adding molecular sieves to the reaction medium was higher (1h of reaction, 51 % conversion) than when the reaction was carried out in the presence of the water scavenger (1h of reaction, 19 % conversion). Similar ee values were obtained in both cases (without 4Å MS, 24 % ee (*R*); with 4Å MS, 23 % ee (*R*)).
- [34] The work-up after quenching was carried out at RT.

- [35] We have not carried out catalytic runs at temperature higher than 298 K because decomposition of the catalyst is apparent above 313 K. Below 223 K the catalytic reaction is too slow.
- [36] Gaussian 09, Revision **D.01**, M. J. Frisch, G. W. Trucks, H. B. Schlegel, G. E. Scuseria, M. A. Robb, J. R. Cheeseman, G. Scalmani, V. Barone, B. Mennucci, G. A. Petersson, H. Nakatsuji, M. Caricato, X. Li, H. P. Hratchian, A. F. Izmaylov, J. Bloino, G. Zheng, J. L. Sonnenberg, M. Hada, M. Ehara, K. Toyota, R. Fukuda, J. Hasegawa, M. Ishida, T. Nakajima, Y. Honda, O. Kitao, H. Nakai, T. Vreven, J. A. Montgomery Jr., J. E. Peralta, F. Ogliaro, M. Bearpark, J. J. Heyd, E. Brothers, K. N. Kudin, V. N. Staroverov, R. Kobayashi, J. Normand, K. Raghavachari, A. Rendell, J. C. Burant, S. S. Iyengar, J. Tomasi, M. Cossi, N. Rega, M. J. Millam, M. Klene, J. E. Knox, J. B. Cross, V. Bakken, C. Adamo, J. Jaramillo, R. Gomperts, R. E. Stratmann, O. Yazyev, A. J. Austin, R. Cammi, C. Pomelli, J. W. Ochterski, R. L. Martin, K. Morokuma, V. G. Zakrzewski, G. A. Voth, P. Salvador, J. J. Dannenberg, S. Dapprich, A. D. Daniels, Ö. Farkas, J. B. Foresman, J. V. Ortiz, J. Cioslowski, D. J. Fox, Gaussian, Inc., Wallingford CT, **2009**.
- [37] a) C. Lee, W. Yang, W. R. G. Parr, *Phys. Rev. B* **1988**, *37*, 785-789. b) A. D. Becke, *J. Chem. Phys.* **1993**, *98*, 1372-1377. c) A. D. Becke, *J. Chem. Phys.* **1993**, *98*, 5648-5652.
- [38] S. Grimme, J. Antony, S. Ehrlich, H. Krieg, *J. Chem. Phys.* **2010**, *132*, 154104.
- [39] F. Weigend, R. Ahlrichs, *Phys. Chem. Chem. Phys.* **2005**, *7*, 3297-3305.
- [40] J. Tomasi, B. Mennucci, R. Cammi, *Chem. Rev.* **2005**, *105*, 2999-3094.
- [41] SAINT+, *version 6.01: Area-Detector Integration Software*, Bruker AXS, Madison, WI, **2001**.
- [42] a) R. H. Blessing, *Acta Crystallogr.* **1995**, *A51*, 33-38. b) SADABS, *Area Detector Absorption Correction Program*, Bruker AXS, Madison, WI, **1996**.
- [43] a) G. M. Sheldrick, *Acta Crystallogr.* **1990**, *A46*, 467-473. b) G. M. Sheldrick, *Acta Crystallogr.* **2008**, *A64*, 112-122.
- [44] G. M. Sheldrick, *Acta Crystallogr.* **2015**, *C71*, 3-8.
- [45] L. J. Farrugia, *J. Appl. Crystallogr.* **2012**, *45*, 849-854.

## Entry for the Table of Contents

## FULL PAPER

Explaining the catalytically selective access to both enantiomers (up to 99 % ee each) of Friedel–Crafts adducts by only changing reaction temperature



Isabel Méndez, Ricardo Rodríguez,\*  
V́ctor Polo, Vincenzo Passarelli,  
Fernando J. Lahoz, Pilar Garća-  
Orduña and Daniel Carmona\*

**Page No. – Page No.**  
Temperature Dual Enantioselective  
Control in a Rhodium–Catalyzed  
Michael Type Friedel–Crafts Reaction:  
A Mechanistic Explanation